ESC European Society of Cardiology

European Heart Journal (2026) **47**, 1702–1717
https://doi.org/10.1093/eurheartj/ehaf349

TRANSLATIONAL SCIENCE
Hypertension

Checkpoint kinase Wee1 activation drives inflammation and hypertrophy through the protein kinase B/phosphoinositide 3-kinases–nuclear factor κB pathway in cardiomyocytes

Mengyang Wang [1,2,3,†], Xue Han [1,4,†], Qinyan Wang [2,†], Tianxiang Yu[2], Wu Luo[2,4], Shiju Ye [5], Xiaochen Guo [2], Zheng Xu [1,4], Zhuqi Huang [2,5], Julian Min[1], Ping Huang[1], Yi Wang [2], and Guang Liang [1,2,4,*]

[1]Department of Pharmacy and Institute of Inflammation, Zhejiang Provincial People's Hospital, Affiliated People's Hospital, Hangzhou Medical College, No. 158 Shangtang Road, Hangzhou, Zhejiang 310014, China; [2]Chemical Biology Research Center, School of Pharmaceutical Sciences, Wenzhou Medical University, No. 1210 University Road, Chashan Higher Education Park, Wenzhou, Zhejiang 325035, China; [3]Department of Pharmacology, College of Pharmacy, Beihua University, Jilin 132013, China; [4]School of Pharmaceutical Sciences, Hangzhou Medical College, No. 481 Binwen Road, Binjiang District, Hangzhou, Zhejiang 310014, China; and [5]Department of Cardiology, Sir Run Run Shaw Hospital, Zhejiang University School of Medicine, Hangzhou, Zhejiang 310020, China

Received 30 July 2024; revised 12 November 2024; accepted 6 May 2025; online publish-ahead-of-print 21 May 2025

See the editorial comment for this article 'AKT and heart remodelling: too much of a good thing?', by R. Wardman and J. Heineke, https://doi.org/10.1093/eurheartj/ehaf506.

Abstract

Background and Aims Hypertensive heart failure has an urgent need for new therapeutic targets. Protein kinases act as key regulators in cellular actions relevant to cardiac pathophysiology. This study identified a protein kinase, Wee1 G2 checkpoint kinase (Wee1), being activated and involved in this disease.

Methods RNA-seq-based kinase enrichment analysis was used to identify the involved kinase pathways. Cardiomyocyte-specific Wee1-deficiency mice with chronic angiotensin II (Ang II) infusion and transverse aortic constriction (TAC) were utilized to develop cardiac remodelling. RNA-seq and co-immunoprecipitation were used to explore the mechanism and substrate of Wee1.

Results Kinase enrichment analysis and experimental evidence revealed that Wee1 phosphorylation at Ser642, but not increased expression, was observed in hypertrophic cardiac tissues from both mice and human patients. Knockdown, pharmacological inhibition, or mutational inactivation of Wee1 significantly alleviated Ang II-induced cardiomyocyte injuries. RNA-seq analysis showed that phosphoinositide 3-kinases/protein kinase B (AKT) pathway mediated the function of Wee1 in cardiomyocytes. Mechanistically, the phosphorylated Wee1 directly binds to the PHD domain of AKT to phosphorylate AKT inducing AKT/phosphoinositide 3-kinases–nuclear factor κB signalling pathway activation and subsequent inflammation and hypertrophy in cardiomyocytes. Cardiomyocyte-specific Wee1 deficiency was found to protect against cardiac inflammation, remodelling, and dysfunction in mice subjected to transverse aortic constriction or Ang II infusion. Pharmacological Wee1 inhibition also attenuated Ang II-induced cardiac remodelling in mice.

Conclusions Cardiomyocyte Wee1 activation drives inflammation and hypertrophy by directly phosphorylating AKT and activating AKT–nuclear factor κB pathway. This study identifies Wee1 as a new upstream kinase of AKT and a potential therapeutic target for hypertensive heart failure.

* Corresponding author. Email: wzmcliangguang@163.com
† The first three authors contributed equally to the study.

Structured Graphical Abstract

Key Question

Are protein kinases involved in hypertensive heart failure?

Key Finding

In a hypertensive mouse model, cardiomyocyte Wee1 G2 checkpoint kinase (Wee1) activation drove inflammation and hypertrophy by directly phosphorylating AKT and activating AKT-NFκB pathway, independent of cell cycle and proliferation regulation. Cardiomyocyte-specific deletion or pharmacological inhibition of Wee1 attenuated hypertensive cardiac remodeling in mice.

Take Home Message

Cardiomyocyte-specific Wee1-AKT/PI3K-NFκB axis plays a key role in regulating cardiac remodeling and is a new potential therapeutic target for hypertensive heart failure.

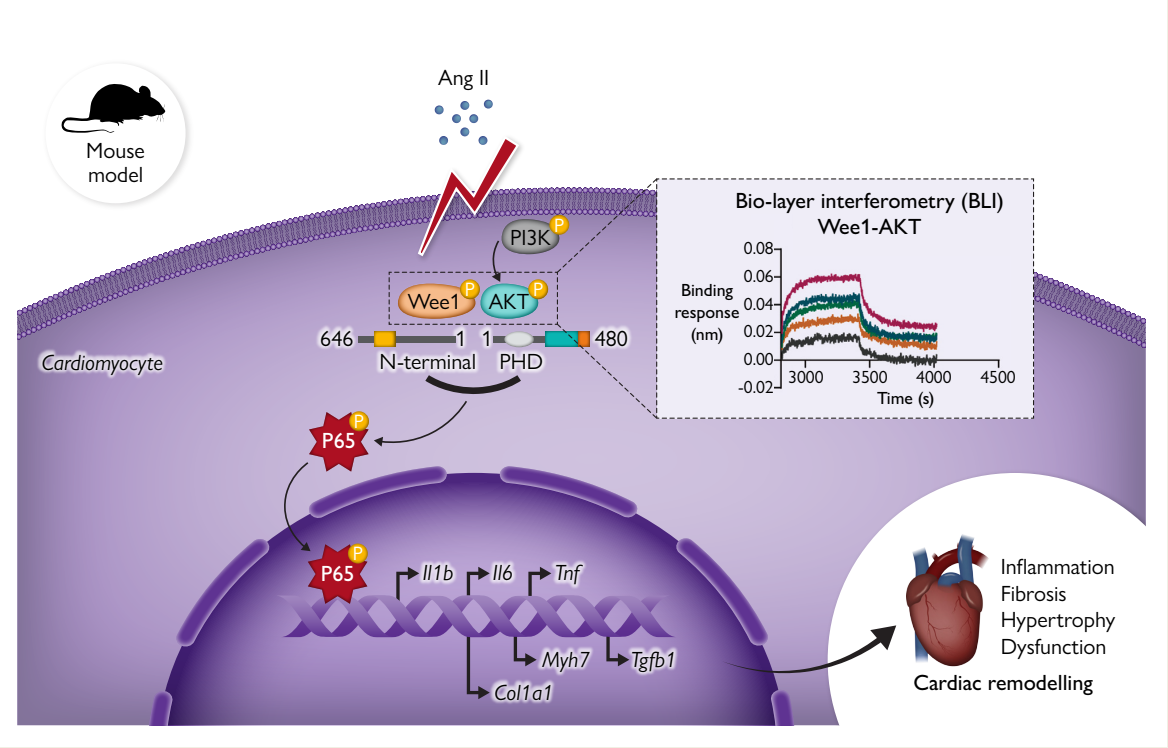

Keywords Wee1 • Protein kinases • AKT • Inflammation • Cardiac remodelling

Translational perspective

This study shows up-regulated Wee1 phosphorylation in hypertrophic cardiomyocytes and presents Wee1 as a new therapeutical target for hypertensive heart failure. Mechanistically, Wee1 activation drives inflammation and hypertrophy by directly phosphorylating protein kinase B (AKT) in cardiomyocytes. Cardiomyocyte-specific deletion or pharmacological inhibition of Wee1 attenuates hypertensive cardiac remodelling in mice. Considering that Wee1 inhibitors have been used in clinical trials for treating cancers, this study suggests that Wee1 inhibitors may expand their applications into hypertensive heart diseases. It is also suggested to develop new small molecules targeting the interaction between Wee1 and AKT to avoid the side effects and treat heart diseases.

Introduction

Hypertension is a persistent and debilitating threat to global public health, remaining the most prominent global driver of cardiovascular disease and mortality.[1] Hypertension can result in myocardial systolic hypokinesis and ventricular remodelling, both of which are central to the pathogenesis of chronic heart failure.[2] Dysregulated angiotensin II (Ang II) signalling activity is a key driver of hypertensive cardiac remodelling.[3] Besides acting in smooth muscle cells to boost blood pressure, the elevated Ang II level could directly trigger inflammation and hypertrophy in cardiomyocytes to induce cardiac injuries and

dysfunction.[4] Although blood pressure can often be controlled with anti-hypertrophic drugs in the clinic, heart failure incidence remains high in hypertensive patients, indicating that other Ang II-related pathways also play an important pathological roles in the development of hypertensive heart complications. Efforts to identify molecular regulators of Ang II-induced cardiomyocyte injuries may thus provide an opportunity to identify new targets for the treatment of hypertensive heart failure.

Protein kinases (PKs) are a large superfamily of proteins that function by phosphorylating the substrate proteins.[5] Protein kinases modulate a wide range of cellular events and pathophysiology and are considered as important targets for drug discovery, especially in cancer treatment. Recently, some PKs are also involved in regulating physiological homeostasis and pathological states in cardiac diseases.[6] For instance, the inhibition of PKD1 has been proposed as a therapeutic approach to protecting against arrhythmia and hypertrophy.[7] Krum *et al.*[8] found that p38 mitogen-activated protein kinase (MAPK) inhibition in rats prevented cardiac remodelling and dysfunction. Rho-associated coiled-coil kinases (ROCKs) also play a role in the pathogenesis of heart failure.[9] Therefore, identify key PKs involved in the hypertensive heart failure may provide new therapeutic targets and drug development for this disease. Interestingly, as pro-phosphorylating enzymes, PKs may predominantly undergo alterations in the kinase activity while maintaining unchanged total expression levels in the pathological state of diseases.[10] Therefore, examining the gene/protein expression level of PKs using conventional RNA-seq, single-cell sequencing, and proteomics could not identify the disease-associated PKs. Kinase enrichment analysis (KEA) of differentially expressed genes from the RNA-sequencing data may provide a good way to identify the activity-changed PKs in diseases.[11]

In the present study, we performed RNA-Seq-based KEA in Ang II-challenged mouse heart tissues and found an activity-increased kinase, Wee1 G2 checkpoint kinase (Wee1), without expression level change, in hypertrophic cardiomyocytes. As we know so far, Wee1 is a serine/threonine kinase and a cell cycle regulator, which phosphorylates cyclin-dependent kinase 1 (CDK1) and other CDKs to regulate G2–M cell cycle progression and DNA damages.[12] Wee1 controls DNA replication, chromosome condensation, and histone transcription.[13] It plays important roles in viral infection,[14] hepatic malaria,[15] and embryonic cardiomyocyte proliferation[16] through its function of regulating cell cycle. Especially, high levels of Wee1 expression and activity are observed in many cancers to promote cancer progresssion.[17,18] Some small-molecule Wee1 inhibitors have been evaluated for pre-clinical and clinical cancer treatment.[19] However, the role of Wee1 in cardiomyocytes and hypertensive heart failure has not yet been studied.

The involvement of Wee1 activity in hypertensive heart failure suggests the new function of Wee1 in non-renewable cardiomyocytes, and demonstrating the role and regulating mechanism of Wee1 in hearts may provide new clinical applications for Wee1 inhibitors. Here, we show that either cardiomyocyte-specific Wee1 knockout or pharmacological inhibition significantly protects hearts against Ang II/transverse aortic constriction (TAC)-induced remodelling and dysfunction in mice. Mechanistically, we illustrate that Wee1 directly interacts with the PHD domain of protein kinase B (AKT) to phosphorylate AKT, inducing AKT/phosphoinositide 3-kinases (PI3K)-nuclear factor κB (NFκB) signalling pathway activation and subsequent inflammation and hypertrophy in cardiomyocytes. Our study illustrates a cardiomyocyte-specific Wee1-AKT/PI3K–NFκB axis in regulating cardiac remodelling and indicates Wee1 as a potential target for heart diseases.

Methods

Detailed methods are described in the Supplementary file. The clinical information and the used RNA sequences are shown in Supplementary data online, *Table S4–7*, respectively.

Results

Cardiomyocyte Wee1 is phosphorylated in hypertrophic cardiac tissue

To explore the kinase signalling pathways related to cardiac remodelling, four RNA-seq datasets from human and mouse heart tissues with pathological cardiac hypertrophy were analysed using KEA approach. The result indicated Wee1, AMPK, AXL, and PLK2 as four kinases whose activation may be related to cardiac remodelling in all four models (*Figure 1A*). Since the AMPK, AXL, and PLK2 pathways have been previously reported to be involved in cardiac remodelling,[20–22] we focused on Wee1 in this study. We also found that the mRNA levels of Wee1 showed no change in hypertrophic hearts compared to that in control hearts (*Figure 1B* and *C*). Serine at 642 (Ser642) is an kinase activity-related phosphorylation site in Wee1.[23] Thus, we observed a significant increase in Ser642 phosphorylation of Wee1 in human hypertrophic heart tissues compared with the healthy heart, without any change in the basal Wee1 protein levels (*Figure 1D* and *E*). Similar results were also obtained in heart tissues of an established mouse model using chronic Ang II infusion (1 μg/kg/min) in mice (*Figure 1F* and *G*).

We then explored the source of p-Wee1 in hearts. Immunofluorescent double-staining analysis of mouse heart tissue showed that p-Wee1-positive cells were cardiomyocytes positive for α-actinin rather than vimentin^{+} fibroblasts (see Supplementary data online, *Figure S1A*). These results were confirmed in isolated neonatal rat ventricular myocytes (NRVMs) and neonatal rat cardiac fibroblasts (NRCFs) treated with Ang II at 1 μM for 2 h, after which western immunoblotting detected high p-Wee1 levels specifically in NRVMs (*Figure 1H* and *I*). When NRVMs were treated with Ang II (1 μM) for various periods of time, a time-dependent increase in Wee1 phosphorylation levels was observed, without any change in total Wee1 levels (see Supplementary data online, *Figure S1B* and *C*). In addition, we found that Ang II-induced Wee1 phosphorylation was mediated by AT1R, since knocking down AT1R reversed Wee1 phosphorylation in Ang II-challenged NRVMs (see Supplementary data online, *Figure S1D*, *Figure 1J* and *K*). These data reveal that cardiomyocyte Wee1 is phosphorylated under pathological conditions and may be involved in cardiac remodelling.

The phosphorylation of Wee1 is involved in the regulation of cardiomyocyte hypertrophy

To explore the role of Wee1 phosphorylation in cardiomyocyte responses, Wee1 phosphorylation in NRVMs was inhibited by siRNA-mediated gene knockdown (see Supplementary data online, *Figure S2A–C*) or pharmacological small-molecule inhibitor MK1775.[24] Knocking down Wee1 in NRVMs was sufficient to suppress the Ang II-induced up-regulation of hypertrophy-associated proteins (β-MyHC) and genes (*Myh7*, *Anp*) (*Figure 2A* and *B*). Phalloidin staining further revealed that silencing Wee1 protected against hypertrophy induced by Ang II (*Figure 2C*, Supplementary data online, *Figure S2D*). MK1775 doses from 0.25 to 80 μM showed no cytotoxic effects on NRVMs (see Supplementary data online, *Figure S2E*), leading to the selection of the 1

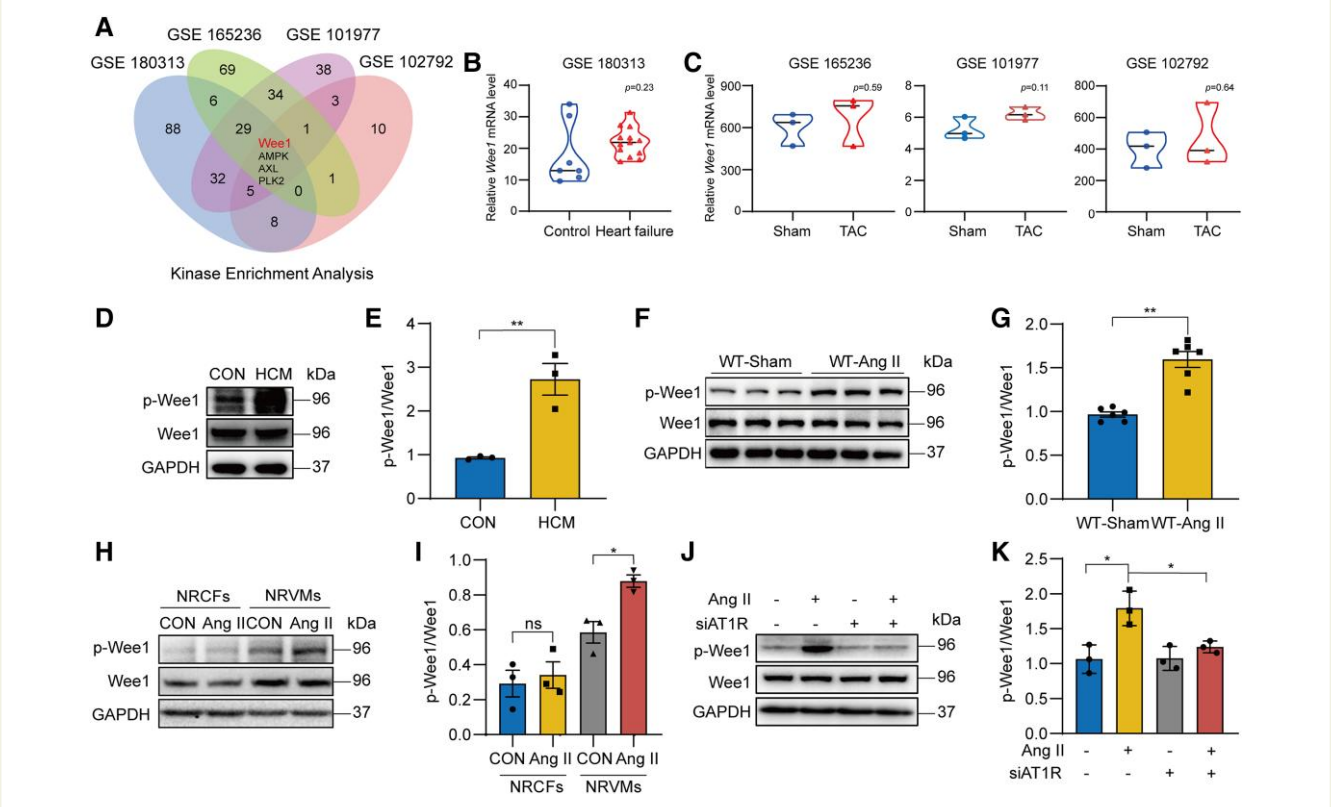

Figure 1 Cardiomyocytes in hypertrophic heart tissues exhibit increased Wee1 phosphorylation. (*A*) A Venn diagram highlighting enriched kinases from four public RNA-seq datasets (GSE102792, GSE165236, GSE101977, and GSE180313). (*B*) *Wee1* mRNA levels in the heart tissues of control and heart failure patients were analysed using a violin plot (GSE180313). (Mean ± SEM; $n = 7$–13). (*C*) *Wee1* mRNA levels in the heart tissues of mice with Sham or transverse aortic constriction surgery were shown in violin plots (GSE102792, GSE165236, and GSE101977). (Mean ± SEM; $n = 3$). (*D*) Representative western blot analyses of p-Wee1 and Wee1 in heart tissue samples from control and hypertrophic cardiomyopathy patient, with glyceraldehyde-3-phosphate dehydrogenase (GAPDH) as a loading control. (*E*) Densitometric quantification of the blots in *D*. (*F*) Angiotensin II was administered to C57BL/6 mice for 4 weeks, after which Wee1 phosphorylation was analysed via western immunoblotting, with each lane representing a separate mouse and GAPDH serving as a loading control. (*G*) Densitometric quantification of the blots in *F*. (*H*) Following treatment for 2 h with angiotensin II (1 μM), neonatal rat ventricular myocytes (NRVMs) and neonatal rat cardiac fibroblasts (NRCFs) were assessed via western immunoblotting to detect p-Wee1 and Wee1, using GAPDH as a loading control. (*I*) Densitometric quantification of the blots in *H*. (*J*) An siRNA construct specific for AT1R was used to transfect NRVMs, followed by angiotensin II treatment (1 μM) for 2 h. Western immunoblotting was then employed to detect p-Wee1 and Wee1, utilizing GAPDH as a loading control. (*K*) Densitometric quantification of the blots in *J*. All data are means ± SEM; $n = 6$; ns, not significant; $^{*}P < .05$; $^{**}P < .01$. $P < .05$ was regarded as significant

and 2.5 μM doses for further *in vitro* use. MK1775 also significantly blocked the up-regulation of hypertrophy-associated genes and proteins in response to Ang II (*Figure 2D and E*), further preventing Ang II-induced cardiomyocyte enlargement (*Figure 2F*, Supplementary data online, *Figure S2F*).

The specific functional importance of the Ser642 phosphorylation of Wee1 in NRVMs was assessed by generating a point mutation at Ser642, establishing two plasmids including a wild-type (WT) Flag-tagged Wee1 ($Wee1^{WT}$) construct and a construct encoding Flag-tagged Wee1 with the inactivating Ser642-Ala mutation ($Wee1^{S642A}$). NRVMs were transfected with the $Wee1^{WT}$ plasmid to increase both basal level and Ser642 phosphorylation of Wee1 (see Supplementary data online, *Figure S2G* and *H*). The overexpression of Wee1 was found to exacerbate the hypertrophic responses of cardiomyocytes to Ang II (*Figure 2G–I*). Next, the $Wee1^{WT}$ and $Wee1^{S642A}$ plasmids were transfected into sgRNA-mediated H9c2 cells without basal Wee1, followed by Ang II treatment for 24 h. The inactivation of Ser642 by S642A mutation ablated Ang II-induced hypertrophic phenotypes in these cardiomyocytes (*Figure 2J and K*, Supplementary data online, *Figure S2I* and *J*), suggesting that the Ser642 phosphorylation is specifically involved in Ang II-induced cardiomyocyte injury. Consistently, we construct a plasmid encoding a phosphomimetic mutant isoform of Wee1 with autoactivating Ser642-Glu mutation, Flag-tagged $Wee1^{S642E}$. When cardiomyocytes without basal Wee1 were transfected with $Wee1^{S642E}$, hypertrophic phenotypes were evidently observed in the absence of Ang II stimulation (*Figure 2L–O*). These data thus offer clear evidence in support of the role that Wee1 Ser642 phosphorylation plays as a mediator of Ang II-induced cardiomyocyte hypertrophy.

Considering that Wee1 is a canonical kinase regulating cell cycle and proliferation,[25] we examined the effects of Ang II and Wee1 on cell cycle of NRVMs using flow cytometry. As shown in the Supplementary data online, *Figure S2K* and *L*, we found that the Ang II challenge for 24 h showed no significant influence on the cell cycle of NRVMs. Then we further examined the cell cycle in NRVMs transfected with siWee1, $Wee1^{WT}$ plasmid, and $Wee1^{S642A}$ plasmid, respectively. The results in the Supplementary data online, *Figure S2M–P* showed that neither silencing Wee1,

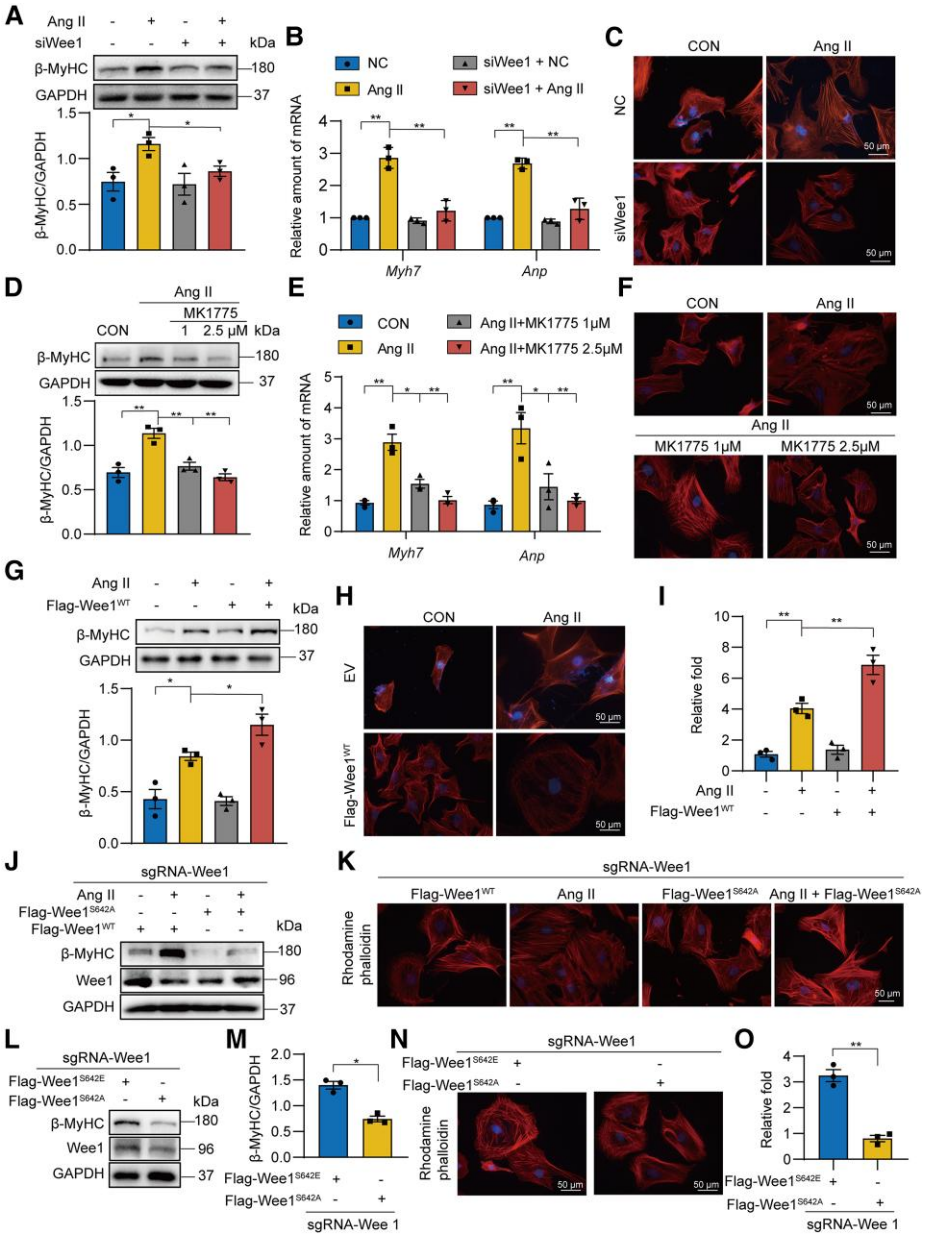

Figure 2 The phosphorylation of Wee1 at Ser642 positively regulates cardiomyocyte hypertrophy. (*A*) Following negative control (NC) or siWee1 transfection, neonatal rat ventricular myocytes (NRVMs) were treated with angiotensin II (1 μM, 24 h), followed by western immunoblotting assay for β-MyHC, using glyceraldehyde-3-phosphate dehydrogenase (GAPDH) as a loading control. (*B*) Following siWee1 transfection, NRVMs were treated with angiotensin II (1 μM, 12 h), and *Myh7* and *Anp* mRNA levels were analysed, using *Actb* for normalization. (*C*) Rhodamine phalloidin and 4',6-diamidino-2-phenylindole (DAPI) staining was used to assess cardiomyocyte size (Scale bar: 50 μm). (*D*) Following pre-treatment with MK1775 (1 or 2.5 μM) for 1 h, NRVMs were treated with angiotensin II (1 μM, 24 h), followed by analyses of β-MyHC via western immunoblotting, using GAPDH as a loading control. (*E*) Following pre-treatment with MK1775 for 1 h, NRVMs were treated with angiotensin II (1 μM, 12 h), and *Myh7* and *Anp* mRNA levels were analysed, using *Actb* for normalization. (*F*) Rhodamine phalloidin and DAPI staining was used to assess cardiomyocyte size (Scale bar: 50 μm). (*G*) After Flag-Wee1 or empty vector (EV) transfection, NRVMs were treated with angiotensin II (1 μM, 24 h), followed by analyses of β-MyHC via western immunoblotting, using GAPDH as a loading control. (*H*) Rhodamine phalloidin and DAPI staining were used to assess cardiomyocyte size (Scale bar: 50 μm). (*I*) Changes in NRVMs size in response to angiotensin II. At least 100 cells from various visual fields were analysed for three samples per group. (*J*) H9c2 cells were transfected with sgRNA-Wee1 to silencing the basal Wee1, and then transfected with Flag-tagged wild type Wee1 ($Wee1^{WT}$) or Flag-tagged $Wee1^{S642}$ constructs, followed by analyses of β-MyHC via western immunoblotting, using GAPDH as a loading control. (*K*) Rhodamine phalloidin and DAPI staining were used to assess cardiomyocyte size (Scale bar: 50 μm). (*L*) sgRNA-Wee1 H9c2 cells were transfected using the $Wee1^{S642A}$ or Flag-tagged Wee1 with Ser-642-Glu ($Wee1^{S642E}$) constructs and cultured for 24 h, after which β-MyHC and Wee1 were detected via western immunoblotting, with GAPDH as a loading control. (*M*) Densitometric quantification of blots in *L*. (*N*) Rhodamine phalloidin and DAPI staining were used to assess cardiomyocyte size (Scale bar: 50 μm). (*O*) Changes in NRVMs size in response to angiotensin II. At least 100 cells from various visual fields were analysed for three samples per group. All data are means ± SEM; $n = 6$; *$P < .05$; **$P < .01$. $P < .05$ was regarded as significant

overexpressing Wee1, nor inactivating Wee1 affected the cell cycle phases of NRVMs. These data indicate that Wee1 does not serve as a cell cycle-regulating kinase in terminally differentiated cardiomyocytes.

Phosphoinositide 3-kinases–protein kinase B signalling pathway mediates the cardiomyocyte hypertrophy induced by the angiotensin II–Wee1 axis

To clarify how Wee1 mediates Ang II-induced hypertrophy, RNA-seq analyses of NRVMs transfected with siWee1 and treated with Ang II were conducted. In total, 58 down-regulated genes and 72 up-regulated genes were observed in the Ang II group relative to the Ang II + siWee1 group (*Figure 3A*). Kyoto encyclopedia of genes and genomes (KEGG) enrichment analyses indicated that the PI3K–AKT pathway was the most strongly enriched for these genes (*Figure 3B*). Nuclear factor κB is a canonical downstream transcriptional factor of the PI3K/AKT pathway,[26] ultimately shaping cellular inflammatory and pathophysiological responses. We found that PI3K/AKT/NFκB p65 was activated in Ang II-challenged NRVMs, while either knockdown or inhibition of Wee1 reversed Ang II-induced PI3K/AKT/p65 phosphorylation (*Figure 3C and D*, Supplementary data online, *Figure S3A* and *B*). Similar trends were observed in the expression profile of p65-target inflammatory factor genes (*Il1b*, *Il6*, and *Tnf*) in NRVMs (see Supplementary data online, *Figure S3C* and *D*). Conversely, overexpressing Wee1 further enhanced PI3K/AKT/p65 phosphorylation in Ang II-challenged cardiomyocytes (*Figure 3E*, Supplementary data online, *Figure S3E*). We then examined the importance of Wee1 Ser642 phosphorylation of Wee1 on the activation of this pathway. Inactivating mutation of $Wee1^{S642A}$ significantly reduced AKT and P65 phosphorylation in Ang II-challenged cardiomyocytes (*Figure 3F and G*). Autoactivating Ser642-Glu mutation of Wee1 induced AKT and P65 phosphorylation in cardiomyocytes (*Figure 3H*, Supplementary data online, *Figure S3F*).

To validate that AKT activation mediates the function of Wee1, a specific AKT inhibitor A674563 and an inactivating mutant of AKT were used to block this pathway. As shown in *Figure 3I–K* and Supplementary data online, *Figure S3G*, AKT inhibitor significantly abrogated P65 phosphorylation and inflammatory and hypertrophic gene up-regulation in NRVMs induced by Ang II challenge and Wee1 overexpression, indicating that AKT mediates cardiomyocyte response to Ang II–Wee1 axis. We also generated a point mutation of AKT at Ser473, the phosphorylating site responsible for AKT activity, establishing two plasmids including wild-type AKT (AKT^{WT}) and Ser473-Ala mutation (AKT^{S473A}). These plasmids were transfected into NRVMs to induce the respective protein overexpression, followed by Ang II treatment for 12 h (see Supplementary data online, *Figure S3H* and *I*). As shown in *Figure 3L and M*, Wee1 overexpression increased the hypertrophic and inflammatory gene expression in AKT^{WT}-containing NRVMs, but failed in AKT^{S473A}-transfected NRVMs, indicating that AKT Ser473 phosphorylation is crucial for Wee1-mediated hypertrophic and inflammatory phenotypes in cardiomyocytes. These results show that Wee1 Ser642 phosphorylation activates PI3K/AKT signalling pathway to induce inflammatory and hypertrophic responses in cardiomyocytes.

Wee1 directly interacts with the PHD domain in protein kinase B to catalyze protein kinase B phosphorylation

We then explored how Wee1 induced PI3K/AKT activation in cardiomyocytes. Wee1 is canonically recognized as an S-G2 checkpoint inhibitor that phosphorylates CDK1 to prevent mitotic entry[27] (see Supplementary data online, *Figure S4A*). Cyclin-dependent kinase 1 is a classic downstream kinase of Wee1. This raised the possibility that Wee1 may activate PI3K/AKT/p65 pathway through CDK1. We silenced CDK1 by siRNA in NRVMs (see Supplementary data online, *Figure S4B* and *C*) and found that silencing CDK1 failed to alleviate Ang II-induced AKT/P65 phosphorylation and hypertrophic and inflammatory gene expression in cardiomyocytes (see Supplementary data online, *Figure S4D–G*), suggesting that Wee1-mediated cardiomyocyte injury is CDK1-independent. These results also promote us to consider if PI3K or AKT is a direct downstream kinase of Wee1. Therefore, the potential ability of Wee1 directly interacting with PI3K or AKT was next investigated in cardiomyocytes (*Figure 4A*).

Interestingly, we found that Wee1 was able to interact with both PI3K and AKT in Ang II-stimulated NRVMs using co-immunoprecipitation (Co-IP) analysis (*Figure 4B*), as well as in cardiac tissues of Ang II-challenged mice (*Figure 4C*). Although PI3K and AKT are mutually causal, we further identified which one is the specific substrate of Wee1 by respectively silencing PI3K or AKT. As shown in *Figure 4D and E*, silencing PI3K failed to affect Wee1–AKT interaction, while silencing AKT blocked Wee1-PI3K complex formation, indicating that AKT is the direct substrate of Wee1. Ang II increased the interaction between Wee1 and AKT/PI3K in cardiomyocytes, while MK1775 dose-dependently suppressed these interactions (*Figure 4F*). A proximity ligation assay (PLA) further visualized Wee1 and AKT interaction in Ang II-challenged NRVMs, while MK1775 suppressed this interaction (*Figure 4G*). Direct Wee1 and AKT protein interaction was further confirmed through a cell-free Bio-layer interferometry (BLI) assay in which the recombinant human Wee1 (rhWee1) and AKT (rhAKT) interacted strongly with a K_D of 1.41×10^{-8} M (*Figure 4H*).

We then explored the specific binding domains for Wee1–AKT interaction. By transfecting HEK-293T cells with plasmids encoding Wee1 and mutant versions of AKT, it was found that Wee1 was unable to bind to an isoform of AKT missing amino acids 5–108 (PHD domain), whereas it could still bind to other AKT mutant proteins (*Figure 4I and J*). Wee1 protein contains a PKD domain and the flexible N-terminal and C-terminal. We constructed a plasmid encoding human influenza hemagglutinin (HA)-Wee1 PHD domain, and however, demonstrated that AKT failed to bind to the PKD domain alone (*Figure 4K and L*). Further study revealed that AKT was unable to bind to Wee1 when the N-terminal in Wee1 was absent (*Figure 4M*). We constructed a plasmid encoding HA-Wee1 N-terminal domain alone and confirmed that AKT bound to the Wee1 N-terminal domain in HEK-293T cells (*Figure 4N*). Further, the $Wee1^{WT}$ and Wee1ΔN plasmids were transfected into H9c2 cells with basal Wee1 deletion by sgRNA-Wee1.The deletion of the N-terminal of Wee1 significantly ablated the ability of Wee1 inducing AKT phosphorylation (*Figure 4O*, Supplementary data online, *Figure S4H*) and hypertrophic and inflammatory gene expression in cardiomyocytes (*Figure 4P and Q*). These data show that the N-terminal in Wee1 and the PHD domain in AKT are responsible to Wee1–AKT interaction and cascade activation.

Finally, we examined if Wee1–AKT interaction afforded AKT phosphorylation using a cell-free assay in the presence of adenosine triphosphate (ATP). In this setting, rhWee1 was found to increase rhAKT phosphorylation dose-dependently, whereas the Wee1 kinase inhibitor MK1775 significantly prevented this phosphorylating effect (*Figure 4R*, Supplementary data online, *Figure S4I*). These results thus demonstrated Wee1 directly interacts with the PHD Domain in AKT through its N-terminal to catalyze AKT phosphorylation (*Figure 4S*).

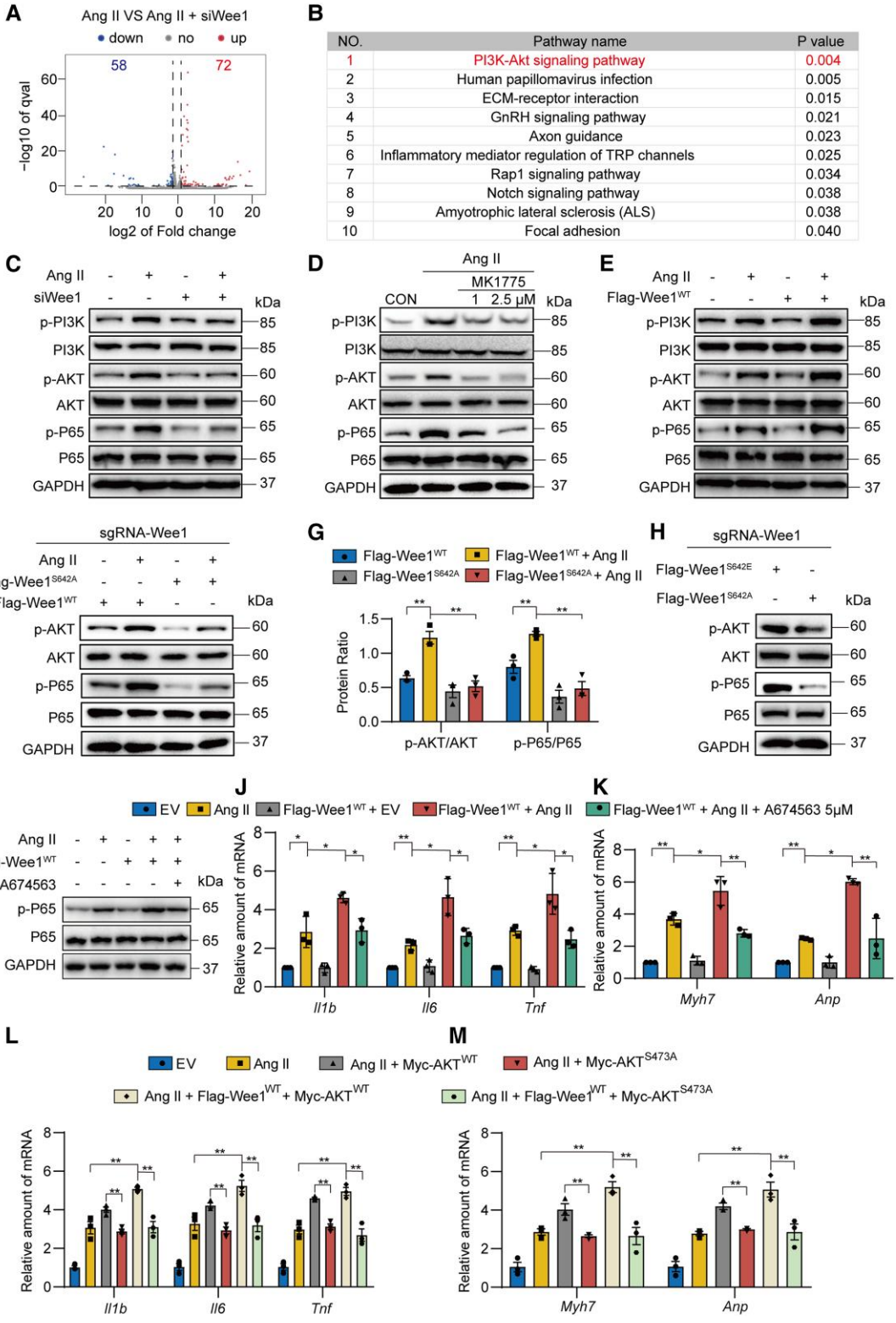

Figure 3 The phosphoinositide 3-kinases–protein kinase B axis is involved in Wee1-mediated cardiomyocyte hypertrophy. (*A*) A volcano plot of genes differentially expressed between the angiotensin II and angiotensin II + siWee1 groups. (*B*) Kyoto encyclopedia of genes and genomes (KEGG) pathways of the RNA-seq data. (*C*) Following negative control siRNA or Wee1 siRNA (siWee1) transfection, neonatal rat ventricular myocytes (NRVMs) were treated with angiotensin II (1 μM, 8 h), and p-PI3K, phosphoinositide 3-kinases, p-AKT, protein kinase B, p-P65, and P65 levels were detected via western immunoblotting, utilizing GAPDH as a loading control. (*D*) Following MK1775 (1 or 2.5 μM) pre-treatment for 1 h, NRVMs were treated with angiotensin II (1 μM, 8 h), and the indicated proteins were detected via western immunoblotting, utilizing glyceraldehyde-3-phosphate dehydrogenase (GAPDH)

Continued

Loss of Wee1 in cardiomyocytes alleviates pathological cardiac remodelling induced by angiotensin II

Tamoxifen-induced cardiomyocyte-specific Wee1 knockout mice (Wee1-CKO) were constructed and used (see Supplementary data online, *Figure S5A*). Wee1 knockout was achieved by intraperitoneally injecting mice with 100 μL of a prepared tamoxifen stock solution every day for 5 days, after which $Wee1^{fl/fl}$ and Wee1-CKO mice were infused with saline or Ang II (1 μg/kg/min) for 4 weeks to induce cardiac remodelling (*Figure 5A*). We also compared the Myh6-Cre^{ERT2} mice and $Wee1^{fl/fl}$ mice under basal or stress conditions, and found no significant difference in cardiac function and heart size (see Supplementary data online, *Figure S5B–F*), indicating that the Cre alone does not affect the cardiac pathophysiology in mice. Western blot assay validated the efficiency of Wee1 deletion in cardiomyocytes of Wee1-CKO mice (see Supplementary data online, *Figure S5G–J*). Cardiomyocyte-specific Wee1 knockout did not affect the profiles of systolic blood pressure and plasma Ang II level in Ang II-infused mice (see Supplementary data online, *Figure S5K* and *L*). However, echocardiography showed that Wee1 deficiency in cardiomyocytes was able to prevent cardiac dysfunction induced by Ang II (*Figure 5B–D*, Supplementary data online, *Table S1*). No increases in the heart weight to body weight or heart weight to tibia weight ratios were observed in these Wee1-CKO mice following Ang II infusion (see Supplementary data online, *Table S1*). Serum atrial natriuretic peptide (ANP) and creatine kinase-myocardial band (CK-MB) levels were elevated in Ang II-induced WT but not Wee1-CKO mice (*Figure 5E and F*). The gross evaluation of mouse heart tissues indicated that Wee1-CKO mice were protected against cardiac hypertrophy induced by Ang II infusion (*Figure 5G*). H&E and wheat germ agglutinin (WGA) staining of these cardiac tissue samples confirmed that structural and hypertrophic changes were evident in $Wee1^{fl/fl}$ mice following Ang II infusion (*Figure 5H and I*, Supplementary data online, *Figure S5M*), whereas such pathological changes were significantly attenuated in Ang II-challenged Wee1-CKO mice. Picro Sirius Red and Masson's Trichrome staining also revealed reduced fibrosis in Ang II-infused Wee1-CKO mice relative to $Wee1^{fl/fl}$ controls (*Figure 5J and K*, Supplementary data online, *Figure S5N* and *O*). Western blot assay also showed that cardiomyocyte-specific Wee1 knockout decreased Ang II-induced overexpression of hypertrophy- and fibrosis-related factors [β-MyHC, ANP, Collagen 1 (COL-1), and transforming growth factor β1 (TGF-β1)] in mouse heart (*Figure 5L*, Supplementary data online, *Figure S5P* and *Q*).

We further examined the levels of AKT/p65 pathway in mouse heart tissues. Wee1-CKO significantly inhibited Ang II-induced AKT/p65 phosphorylation and inflammatory gene transcription in mouse hearts (*Figure 5M and N*, Supplementary data online, *Figure S5R–T*). We also examine the mRNA expression of chemokines (*Il8, Mcp-1*, *Icam-1*, and *Vcam-1*) and inflammatory cell ($F4/80^+$ and $CD86^+$) infiltration in mouse heart tissues, showing that cardiomyocyte-specific Wee1 deficiency significantly inhibit Ang II-induced cardiac chemokine levels and macrophage infiltration (see Supplementary data online, *Figure S5U* and *V*). Together, these data demonstrate that Wee1 deficiency in cardiomyocytes protects against cardiac remodelling in Ang II-infused mice. By the way, we performed the immunofluorescence staining of Wee1 and AKT using mouse heart tissues and confirmed that Wee1 was able to interact with AKT in cardiac tissues of Ang II-challenged mice (see Supplementary data online, *Figure S5W*).

Pharmacological inhibition of Wee1 kinase also protects against angiotensin II-induced cardiac remodelling in mice

Wild-type mice were infused with saline or Ang II (1 μg/kg/min) for 4 weeks, administering two MK1775 doses beginning 2 weeks after the start of Ang II infusion (*Figure 6A*). The doses of MK1775 at 20 and 50 mg/kg were selected based on the prior reports[28,29] and dose-dependently inhibited Wee1 phosphorylation in Ang II-challenged mouse hearts (see Supplementary data online, *Figure S6A* and *B*). Angiotensin II infusion increased systolic blood pressure and serum Ang II level in mice, and MK1775 had no effect on these two indexes (see Supplementary data online, *Figure S6C* and *D*). Through non-invasive echocardiography, MK1775 was found to alleviate Ang II-induced cardiac dysfunction in a dose-dependent fashion, as evidenced by the reversed ejection fraction (EF) and fractional shortening (FS) values in MK1775-treated hypertensive mice (*Figure 6B–D*, Supplementary data online, *Table S2*). MK1775 treatment also prevented the increases in the serum levels of CK-MB and ANP in mice challenged with Ang II (*Figure 6E and F*). Comprehensive histological examination showed that MK1775 prevented Ang II-induced cardiac hypertrophy and fibrosis (*Figure 6G–K*, Supplementary data online, *Figure S6E–G*). MK1775 also normalized the up-regulation of hypertrophy- and fibrosis-related factors in Ang II-challenged mouse hearts (*Figure 6L*, Supplementary data online, *Figure S6H* and *I*). As expected, MK1775 treatment inhibited the AKT and p65 phosphorylation (*Figure 6M and N*, Supplementary data online, *Figure S6J* and *K*), inflammatory gene expression (see Supplementary data online, *Figure S6L* and *M*), and inflammatory cell infiltration (see Supplementary data online, *Figure S6N*) in Ang II-infused cardiac tissues. Finally, MK1775 treatment inhibited the Wee1-AKT interaction in Ang II-infused cardiac tissues (see Supplementary data online, *Figure S6O*). These data show that MK1775 inhibits

Figure 3 Continued

as a loading control. (*E*) Following Flag-Wee1 or empty vector (EV) transfection, NRVMs were treated with angiotensin II (1 μM, 8 h), and the indicated proteins were detected via western immunoblotting, utilizing GAPDH as a loading control. (*F*) sgRNA-Wee1 H9c2 cells were transfected with the Flag-tagged $Wee1^{WT}$ or Flag-tagged $Wee1^{S642A}$ followed by angiotensin II treatment (1 μM, 8 h), and the indicated proteins were detected via western immunoblotting. (*G*) Densitometric quantification of the blots in *F*. (*H*) Following the transfection of sgRNA-Wee1 H9c2 cells with $Wee1^{S642A}$ or Flag-tagged $Wee1^{S642E}$ constructs, cells were cultured for 8 h, and p-AKT, protein kinase B, p-P65, and P65 were detected by western immunoblotting with GAPDH as a loading control. (*I–K*) Following Flag-Wee1 or EV transfection, NRVMs were pre-treated with A674563 and then challenged by angiotensin II (1 μM, for 8 h). p-AKT/protein kinase B and p-P65/P65 were detected by western blotting with GAPDH as a loading control (*I*), and the inflammatory gene (*J*) and hypertrophy-related gene (*K*) mRNA levels were assessed by qPCR, with *Actb* for normalization. (*L* and *M*) AKT^{WT} and AKT^{S473A} plasmids, as well as the $Wee1^{WT}$ plasmid, were transfected into NRVMs, respectively, followed by angiotensin II treatment for 12 h and then the mRNA levels of inflammatory genes (*L*) and hypertrophy-related genes (*M*) were detected by qPCR. Data were normalized to *Actb*. All data are means ± SEM; $n = 6$; $^*P < .05$; $^{**}P < .01$. $P < .05$ was regarded as significant

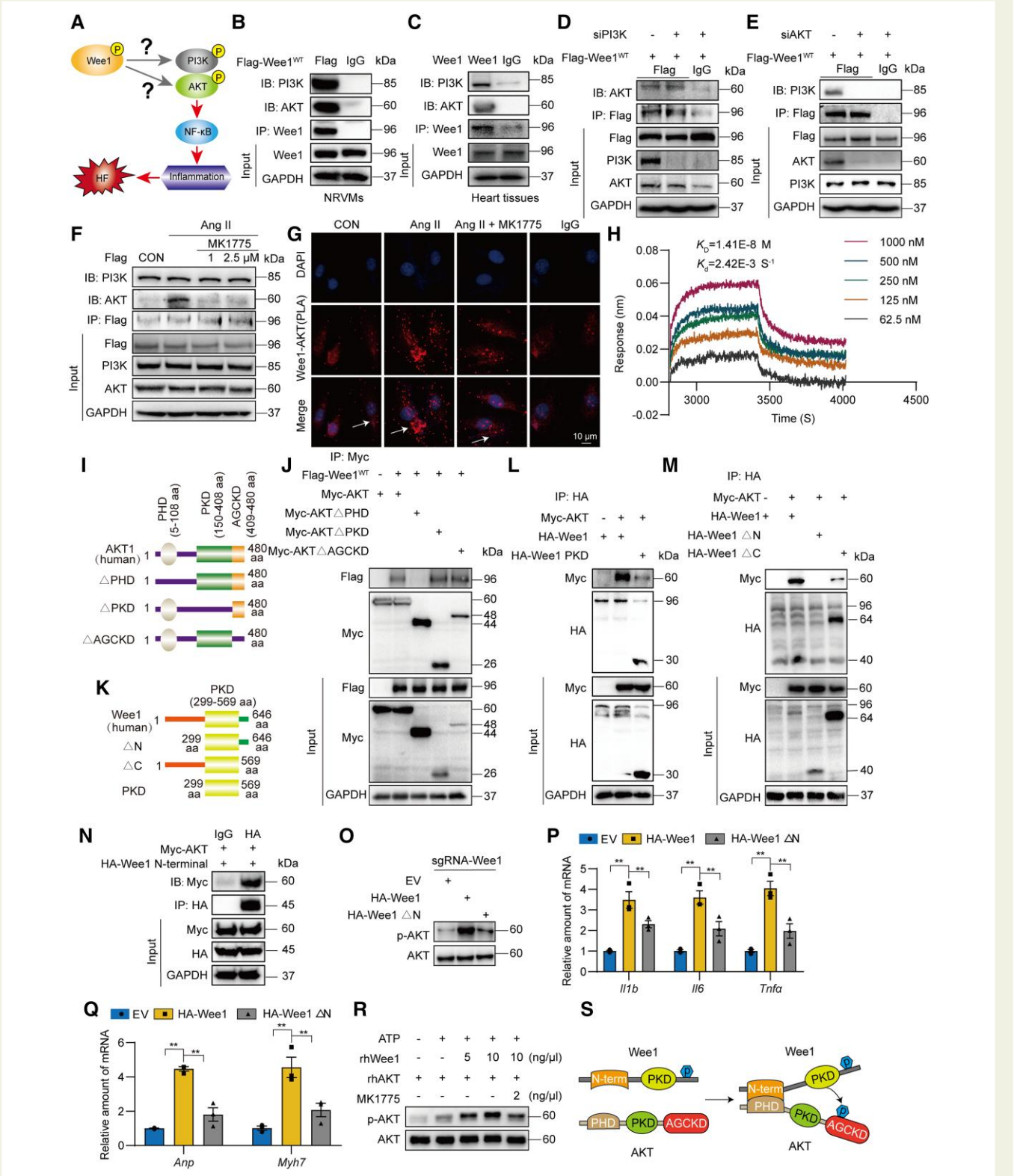

Figure 4 The N-terminal of Wee1 can directly interact with the protein kinase B PHD domain. (*A*) A working model of the proposed ability of Wee1 to regulate phosphoinositide 3-kinases or protein kinase B. (*B*) Following Flag-Wee1 transfection, neonatal rat ventricular myocytes (NRVMs) were lysed, precipitated with anti-Flag (or IgG control), and phosphoinositide 3-kinases and protein kinase B were detected via immunoblotting. (*C*) Anti-Wee1 or control IgG were used to immunoprecipitate murine cardiac tissue lysates, followed by the detection of phosphoinositide 3-kinases and protein kinase B by immunoblotting. (*D*) Following siPI3K transfection, NRVMs were transfected with a plasmid to overexpress Flag-Wee1, after which interactions between Wee1 and protein kinase B were assessed using co-immunoprecipitation. (*E*) Following siAKT transfection, NRVMs were transfected with a plasmid to overexpress Flag-Wee1, after which interactions between Wee1 and phosphoinositide 3-kinases were

Continued

Wee1–AKT cascade and prevents cardiac remodelling in Ang II-challenged mice.

Cardiomyocyte-specific Wee1 deficiency protects against transverse aortic constriction-induced cardiac remodelling

Finally, we tried to determine whether Wee1 deficiency prevents cardiac remodelling in other mouse model. To test this, we performed TAC in both $Wee1^{fl/fl}$ and Wee1-CKO mice after tamoxifen injection (*Figure 7A*). Similarly, Cre alone does not affect the cardiac pathophysiology in the sham or TAC mice (see Supplementary data online, *Figure S7A–E*). Transverse aortic constriction operation increased cardiac p-Wee1 level in $Wee1^{fl/fl}$ mice but not in Wee1-CKO mice (see Supplementary data online, *Figure S7F* and *G*). Similar to our studies using Ang II-challenged mice, cardiomyocyte-specific Wee1 deficiency protected against cardiac dysfunction in TAC mice (*Figure 7B–D*, Supplementary data online, *Table S3*). Relative to sham controls, $Wee1^{fl/fl}$-TAC mice showed significant increases in serum CK-MB and ANP levels, while these increases were normalized in Wee1-CKO-TAC mice (*Figure 7E* and *F*). Cardiomyocyte Wee1 deletion also markedly alleviated cardiac hypertrophy and fibrosis in TAC model mice (*Figure 7G–L*, Supplementary data online, *Figure S7H–L*), accompanied with the reduced levels of AKT/P65 phosphorylation in TAC-treated mice (*Figure 7M* and *N*, Supplementary data online, *Figure S7M* and *N*). Similar changing profiles were observed when we examined inflammatory markers (see Supplementary data online, *Figure S7O–Q*).

Previous studies reported that TAC surgery or Ang II infusion in mice induced a small proportion of DNA damage in cardiac cells.[30,31] We performed TUNEL staining to detect DNA damage in TAC mouse heart tissues and showed that TAC induces <4% TUNEL-positive cardiomyocytes with DNA damage, while the absence of Wee1 did not affect the DNA damage profile induced by TAC (see Supplementary data online, *Figure S8A*). Similar results were observed in Ang II-challenged mouse heart tissues and cultured NRVMs (see Supplementary data online, *Figure S8B* and *C*). In addition, stressed cells may enter a senescent state,[32] which could contribute to tissue inflammation and dysfunction. To examine the effect of Wee1 on cardiomyocyte senescence, we examined the levels of senescent cell markers, P16 and P21,[33] in both heart tissues and cardiomyocytes. The results showed that TAC or Ang II-induced the up-regulation of P16 and P21 in both mouse heart tissues and cultured NRVMs, respectively. However, the absence of Wee1 did not attenuate the TAC or Ang II-induced increases in P16 and P21 levels (see Supplementary data online, *Figure S8D–F*), indicating that Wee1 did not regulate the cellular senescence in cardiomyocytes. These data confirmed that cardiomyocyte-specific Wee1 deficiency protected against TAC-induced cardiac remodelling, which is independent of regulating DNA damage and cardiomyocyte senescence.

Discussion

This study offers new, mechanistic insights into the role that Wee1 plays in the context of cardiac inflammation and remodelling induced by Ang II. Significant increase in Wee1 phosphorylation but not expression was observed in hypertrophic cardiac tissues from mice and humans, particularly in cardiomyocytes. *In vitro* analyses revealed that Wee1 Ser642 phosphorylation was able to mediate Ang II-induced cardiomyocyte hypertrophy. RNA-seq analyses revealed a role of the PI3K–AKT pathway in the function of Wee1, and the N-terminal of Wee1 was ultimately found to interact with the AKT PHD domain. The knockout of Wee1 in cardiomyocytes was sufficient to protect against Ang II-induced cardiac dysfunction and hypertrophy in mice, and pharmacologically inhibiting Wee1 also significantly alleviated cardiac inflammation, remodelling, and dysfunction in response to Ang II. These results thus establish Wee 1 as a promising target for future efforts to develop drugs aimed at treating heart failure.

Wee1 is a canonical kinase regulating cell cycle and proliferation and plays an important role in tumorgenesis. Here, we found an increase of p-Wee1 (Ser642) level in the hearts of Ang II-infused mice and in hypertrophic cardiac tissue from humans, without any change in total Wee1 level. We further demonstrate cardiomyocyte Wee1 as an important regulating kinase in cardiac remodelling through directly phosphorylating AKT. This new biofunction of Wee1 attributes to its Ser642 phosphorylation, as evidenced by our studies using inactivating Ser642-Ala and auto-activating Ser642-Glu mutations. In fact, the classical cell cycle-regulating function of Wee1 also depends on its Ser642 phosphorylation. Phosphorylation of Wee1 at Ser642 is critical event triggered by DNA damage, which induces or maintains cell cycle arrest. DNA damage

Figure 4 Continued

assessed using co-immunoprecipitation. (*F*) Following a 1 h pre-treatment with MK1775 (1 or 2.5 μM), NRVMs were treated with angiotensin II (1 μM, 1 h), followed by Flag-Wee1 plasmid transfection. Interactions between Wee1 and protein kinase B or phosphoinositide 3-kinases were then assessed using co-immunoprecipitation. (*G*) The interaction between protein kinase B and Wee1 was detected by proximity ligation assay assay. Cells were counterstained with 4',6-diamidino-2-phenylindole (DAPI). Arrows showing proximity. (*H*) Bio-layer interferometry (BLI) analyses indicated a direct interaction between Wee1 and protein kinase B, with the presented association and dissociation constants being means from three independent experiments. (*I*) Schematic overview of the prepared protein kinase B domain deletion constructs. (*J*) Protein kinase B, AKTΔPHD, AKTΔPKD, AKTΔAGCKD, and Wee1 were co-transfected in HEK-293T cells using Myc-AKT, Myc-AKTΔPHD, Myc-AKTΔPKD, Myc-AKTΔAGCKD, and Flag-Wee1 constructs, after which Myc antibodies were used for immunoprecipitation followed by probing for Wee1. (*K*) Schematic overview of the prepared Wee1 deletion constructs. (*L*) After transfecting HEK-293T cells with human influenza hemagglutinin (HA)-tagged full-length Wee1, HA-Wee1 PKD constructs, and Myc-protein kinase B, anti-HA was used to perform co-immunoprecipitation. (*M*) After transfecting HEK-293T cells with HA-tagged full-length Wee1, HA-Wee1ΔN, HA-Wee1ΔC constructs, and Myc-protein kinase B, anti-HA was used to perform co-immunoprecipitation. (*N*) After transfecting HEK-293T cells with HA-Wee1 N-terminal domain construct, Myc-protein kinase B and anti-HA were used to perform co-immunoprecipitation. (*O*) Following the transfection of sgRNA-Wee1, H9c2 cells were transfected with HA-Wee1 or HA-Wee1ΔN constructs for 8 h, and p-AKT and protein kinase B were detected by western immunoblotting. (*P* and *Q*) Following the transfection of sgRNA-Wee1, H9c2 cells were transfected with HA-Wee1 or HA-Wee1ΔN constructs for 12 h, the mRNA levels of *Il1b*, *Il6*, *Tnf*, *Myh7*, and *Anp* were detected by qPCR. Data were normalized to *Actb*. (*R*) rhWee1 and rhAKT proteins were incubated together with adenosine triphosphate (ATP) and Wee1 inhibitor MK1775, followed by the immunoblotting-based detection of protein kinase B phosphorylation ($n = 3$). (*S*) Working model detailing the proposed interactions between Wee1 and protein kinase B. All data are means ± SEM; $n = 6$; $^{**}P < .01$. $P < .05$ was regarded as significant

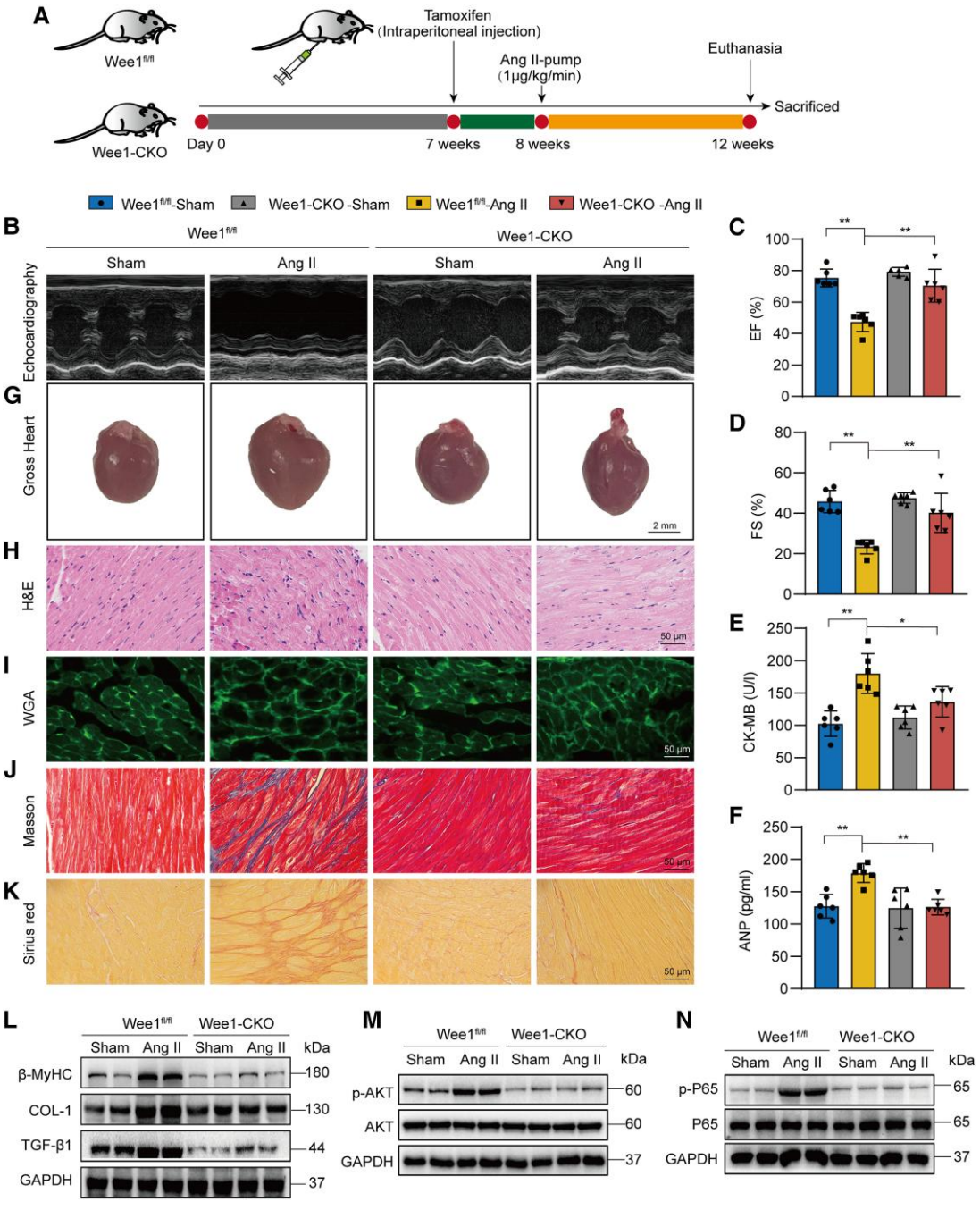

Figure 5 Wee1 deficiency in cardiomyocytes protects hearts against pathological remodelling and inflammation induced by angiotensin II. (*A*) A mouse study flowchart demonstrating angiotensin II and tamoxifen treatment. (*B*) Representative echocardiographic images from animals in the indicated groups. (*C* and *D*) Cardiac functional test results showing ejection fraction and fractional shortening. (*E* and *F*) Serum creatine kinase-myocardial band (CK-MB) (*E*) and atrial natriuretic peptide (ANP) (*F*) levels in the indicated mice. (*G*) Representative images of the whole heart tissue (Scale bar: 2 mm). (*H*) H&E-stained cardiac tissue samples (Scale bar: 50 μm). (*I*) Fluorescently conjugated wheat germ agglutinin (WGA) was used to stain cardiac tissue samples as a measure of cardiomyocyte hypertrophy (Scale bar: 50 μm). (*J* and *K*) Masson's Trichrome (*J*) and Picro Sirius Red (*K*) staining were used to assess cardiac fibrosis (Scale bar: 50 μm). (*L*–*N*) Representative western immunoblotting analyses of cardiac β-MyHC, Collagen 1, and transforming growth factor β1 (*L*), p-AKT and protein kinase B (*M*), or p-P65 and P65 (*N*) levels, with glyceraldehyde-3-phosphate dehydrogenase (GAPDH) as a loading control. All data are means ± SEM; $n = 6$; *$P < .05$; **$P < .01$. $P < .05$ was regarded as significant

induces the cell cycle checkpoint kinase CHK1 to catalyze Wee1 Ser642 phosphorylation.[34] The down-regulation of PTEN in cells treated with genistein led to increases in p-Wee1 (Ser642) level, culminating in decreased G2/M cell cycle arrest.[35] Although our data showed that silencing AT1R reversed Wee1 phosphorylation at Ser642 in Ang II-challenged NRVMs, the mechanism by which Ang II-AT1R axis

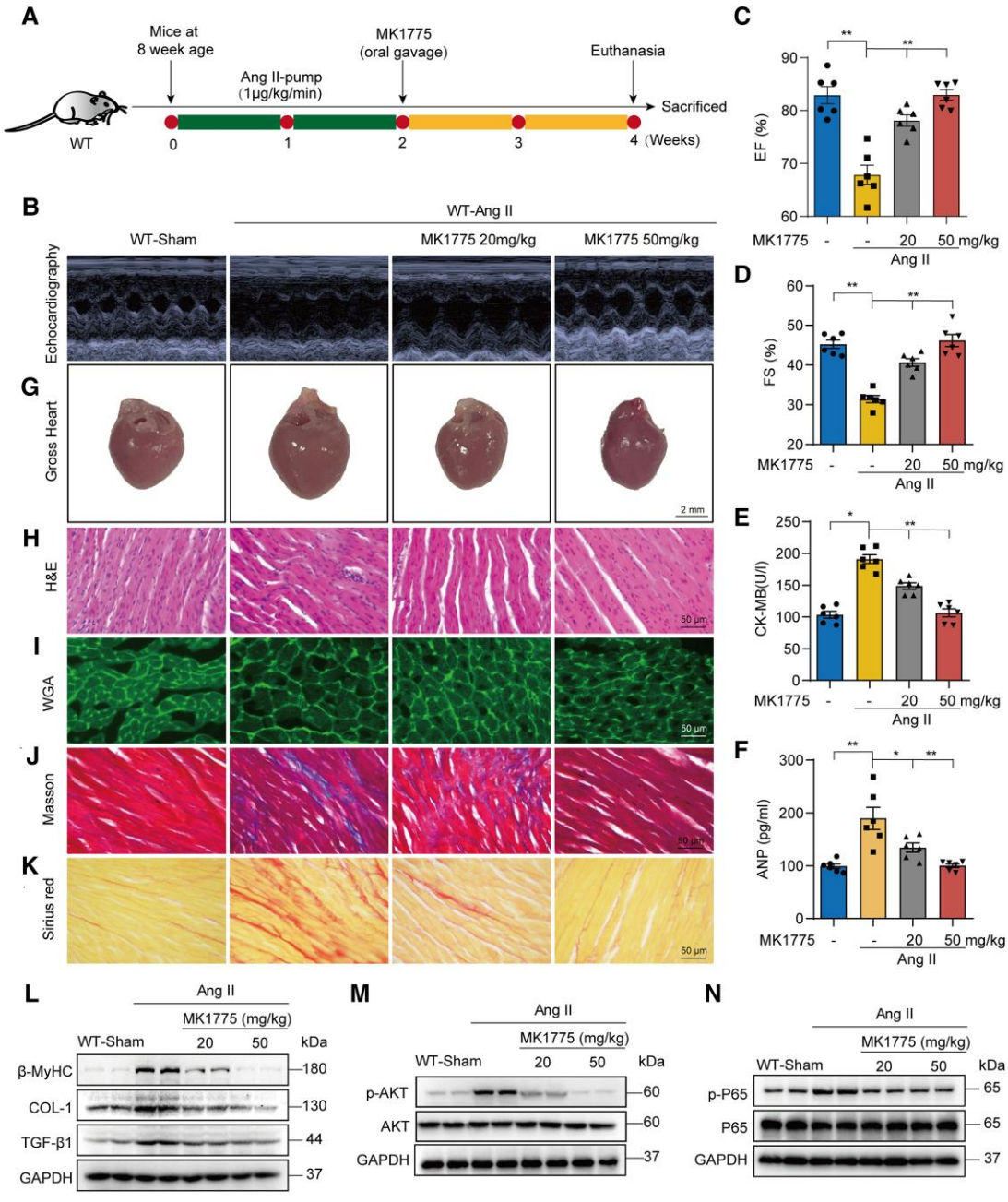

Figure 6 Wee1 inhibitor MK1775 protects hearts against angiotensin II -induced pathological remodelling and inflammation. C57BL/6 mice were infused with saline (Sham) or angiotensin II for 4 weeks. Beginning at Week 2 of angiotensin II treatment, MK1775 was used to treat mice. (*A*) Animal study flowchart. (*B*) Representative echocardiographic images from animals in the indicated groups. (*C* and *D*) Cardiac functional test results showing ejection fraction and fractional shortening. (*E* and *F*) Serum creatine kinasemyocardial band (CK-MB) (*E*) and atrial natriuretic peptide (ANP) (*F*) levels in the indicated mice. (*G*) Representative images of the whole heart tissue (Scale bar: 2 mm). (*H*) H&E-stained cardiac tissue samples (Scale bar: 50 μm). (*I*) Fluorescently conjugated wheat germ agglutinin (WGA) was used to stain cardiac tissue samples as a measure of cardiomyocyte hypertrophy (Scale bar: 50 μm). (*J* and *K*) Masson's Trichrome (*J*) and Picro Sirius Red (*K*) staining were used to assess cardiac fibrosis (Scale bar: 50 μm). (*L–N*) Representative western immunoblotting analyses of cardiac β-MyHC, Collagen 1, and transforming growth factor β1 (*L*), p-AKT and protein kinase B (*M*), or p-P65 and P65 (*N*) levels, with glyceraldehyde-3-phosphate dehydrogenase (GAPDH) as a loading control. All data are means ± SEM; $n = 6$; ns, $^{*}P < .05$; $^{**}P < .01$. $P < .05$ was regarded as significant

mediates Wee1 phosphorylation deserves further investigation in the future.

An interesting concern is that Wee1 has been widely reported to regulate cell cycle in differentiable cells, while a majority of cardiomyocytes are terminally differentiated. Adult cardiomyocytes show very limited proliferative capacity and cell cycle activity.[36] Cardiomyocyte cell cycle activity peaks at post-natal Day 2 and rapidly declines thereafter, with almost all cardiomyocytes arrested at the G1/S cell cycle transition.[37] We utilized

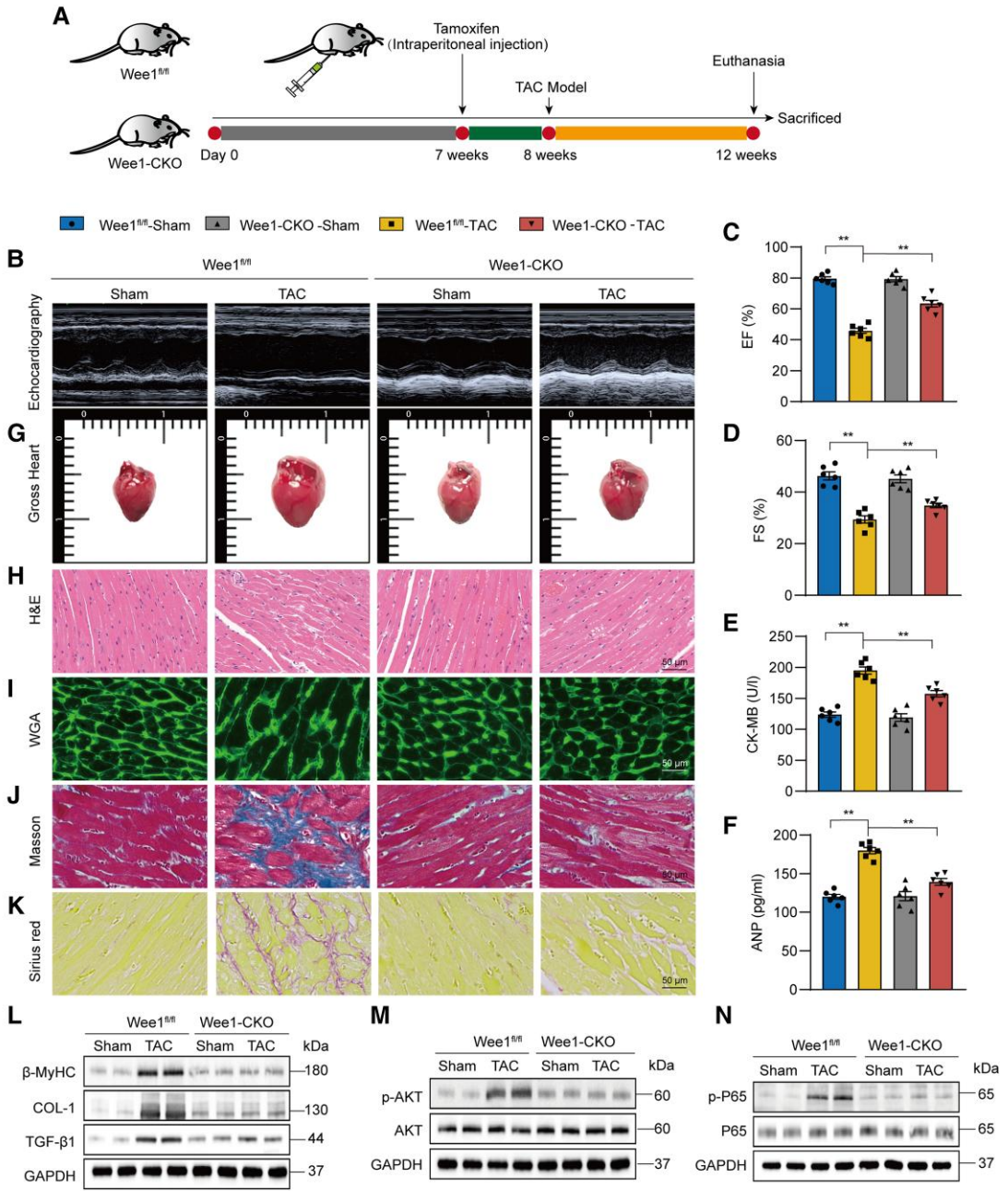

Figure 7 Cardiomyocyte Wee1 deficiency attenuates pathological remodelling and inflammation in transverse aortic constriction mice. Wee1 was knocked out in murine cardiomyocytes through intraperitoneal tamoxifen injections on 5 consecutive days. The resultant Wee1$^{fl/fl}$ and cardiomyocyte-specific Wee1 knockout mice then underwent transverse aortic constriction surgery. (*A*) A study flowchart. (*B*) Representative echocardiographic images from animals in the indicated groups. (*C* and *D*) Cardiac functional test results showing ejection fraction and fractional shortening. (*E* and *F*) Serum creatine kinasemyocardial band (CK-MB) (*E*) and atrial natriuretic peptide (ANP) (*F*) levels in the indicated mice. (*G*) Representative images of the whole heart tissue (Scale bar: 2 mm). (*H*) H&E-stained cardiac tissue samples (Scale bar: 50 μm). (*I*) Fluorescently conjugated WGA was used to stain cardiac tissue samples as a measure of cardiomyocyte hypertrophy (Scale bar: 50 μm). (*J* and *K*) Masson's Trichrome (*J*) and Picro Sirius Red (*K*) staining were used to assess cardiac fibrosis (Scale bar: 50 μm). (*L–N*) Representative western immunoblotting analyses of cardiac β-MyHC, Collagen 1, and transforming growth factor β1 (*L*), p-AKT and protein kinase B (*M*), or p-P65 and P65 (*N*) levels, with glyceraldehyde-3-phosphate dehydrogenase (GAPDH) as a loading control. All data are means ± SEM; $n = 6$; $^{*}P < .05$; $^{**}P < .01$. $P < .05$ was regarded as significant

the adult mouse hearts and primary NRVMs obtained from 5-day-old rats. Therefore, it is likely that only a limited number of these cardiomyocytes exhibited low cell cycle activity. Our data also confirmed that neither Ang II challenge nor Wee1 change affects cell cycle activity in NRVMs, indicating that Wee1 loses its classical function as a cell cycle regulator in adult cardiomyocytes. In addition, stressed and hypertrophic cardiomyocytes may experience the endoreplication or endomitosis stages, where cardiomyocytes replicate their DNA and increase their size without completing cytokinesis and dividing.[38,39] It is unclear if the Wee1 activation regulates endoreplication or endomitosis in cardiomyocyte to promote

hypertrophy, which deserves further investigation. However, this possible regulation on endoreplication or endomitosis did not contribute to the cell cycle activity of adult cardiomyocytes. In addition, Ang II infusion or TAC surgery induced a small proportion of DNA damage in hearts.[30,31] Aime-Sempe *et al.*[40] found a few DNA breaks in heart tissues of patients with congestive heart failure disease. However, our data demonstrate that Wee1 deletion does not affect DNA damage profile in stressed hearts and cardiomyocytes. Together, this study shows that Ser 642 phosphorylation of Wee1 promotes inflammation and remodelling via AKT–NFκB pathway in terminally differentiated cardiomyocytes, which is independent of cell cycle regulation.

RNA-seq analyse showed that the PI3K–AKT signalling pathway was involved in Wee1-mediated cardiomyocyte injuries. It has been reported that PI3K–AKT signalling serves as a regulating pathway for the inflammation and hypertrophy in cardiomyocytes.[41] The traditional herbal medicine Qingda granule has also been demonstrated to protect against Ang II-induced cardiac hypertrophy and damage through modulation of PI3K/AKT pathway.[42] In addition to hypertrophy, PI3K/AKT may also mediate chronic inflammation in the heart.[43] The overexpression and activation of AKT were found to be detrimental to cardiac function. This has been further demonstrated by reports in which ablation of AKT prevented increased cell size and cardiac dysfunction.[44] After activation, AKT promotes cell inflammation, proliferation, cell cycle, and antiapoptosis by phosphorylating and activating its numerous downstream targets, including NFκB, AP-1, GSK3, Bad, FOXO, mTOR, and HIF-1.[45] Nuclear factor κB is a canonical downstream transcriptional factor of the PI3K–AKT pathway.[26] phosphoinositide 3-kinases–AKT controls NFκB activity and thereby regulates inflammatory responses.[24] Suppressing the PI3K–AKT/NFκB-induced inflammatory responses safeguarded heart hypertrophy in Ang II-stimulated mice.[46] Small molecule PI3K or AKT inhibitors, including LY294002 (PI3K inhibitor),[47] TG100-115 (PI3K inhibitor),[48] and A674563 (AKT inhibitor),[49] have been reported to prevent cardiac injury in animal models. However, since the distribution of PI3K and AKT lacks the tissue specificity, PI3K/AKT inhibitors may influence the physiological function in normal tissues and then possess potential risks. Here, we demonstrate that Wee1 is phosphorylated in the pathological state of cardiac hypertrophy and then activate AKT–NFκB signalling pathway to promote cardiomyocyte injuries. This finding provides Wee1 inhibition as a new avenue to regulate AKT activity and protect hearts.

A new finding of this study is that Wee1 directly phosphorylates AKT to induce AKT activation. Previous study has reported that Wee1 phosphorylates CDK1.[50] However, we found that CDK1 knockdown could not affect Ang II-induced AKT/P65 phosphorylation and remodelling phenotypes in cardiomyocytes, suggesting that CDK1 is not involved in cardiomyocyte injuries. These results promote us to consider if PI3K or AKT is a direct and new substrate of Wee1. Although PI3K and AKT are mutually causal, we further confirmed that AKT is a direct substrate of Wee1 in cardiomyocytes. AKT exists in three isoforms including AKT1, AKT2, and AKT3.[51] While only AKT1 expression is broadly observed across tissue types, AKT2 is largely restricted to the fat and muscle cells and AKT3 expression is mostly observed in the brain and testes. The PH domain of AKT1 exhibits strong affinity and selectivity for phosphatidylinositol 34,5-triphosphate (PIP3) through interactions with positively charged basic residues.[52] The binding of PIP3 has been suggested to primarily drive cellular signalling through direct and allosteric activation of AKT kinase activity.[53] Considering that the direct upstream kinase of AKT remains unclear, this study clearly identifies Wee1 as a kinase directly phosphorylating AKT. It will be interesting to examine if Wee1 also phosphorylates AKT in cancer cells and regulates AKT-mediated cellular biology under other pathophysiological conditions.

Wee1 is a tyrosine kinase that regulates mitotic entry such that, when deleted, results in pre-implantation lethality in mice. Mouse cells harbouring Wee1 mutations fail to complete mitosis and exhibit a range of defects tied to mitotic dysregulation such that genomic integrity is compromised with progression through mitosis.[54] Here, this embryonic lethality was bypassed through the generation of tamoxifen-inducible cardiomyocyte-specific Wee1 knockout mice. The role of Wee1 in certain cancers makes targeting Wee1 using specific small-molecule inhibitors including MK1775 as an anti-cancer strategy.[55] MK1775 has been shown to increase the radiosensitivity of lung, breast, skin, brain, and prostate cancer cells to agents that induce DNA damage.[56] In this study, oral intake of MK1775 (20 or 50 mg/kg, 14 days) showed no toxic phenotypes and was sufficient to rescue Ang II-induced cardiac hypertrophy, fibrosis, and inflammatory activity. These data indicate that pharmacological inhibition of Wee1 could protect hearts and the anti-cancer Wee1 inhibitors may expand their applications into heart diseases. However, as a Wee1 inhibitor regulating cell cycle, MK1775 showed the gastrointestinal reaction side-effect in its clinical trials treating cancers.[57] Therefore, it is suggested to develop new small molecules targeting the interaction between Wee1 and AKT to avoid the side-effects and treat heart diseases.

Conclusions

In conclusion, this study found up-regulated Wee1 phosphorylation in cardiomyocytes in hypertensive heart tissues and showed that cardiomyocyte-specific deletion or pharmacological inhibition of Wee1 attenuated Ang II-induced cardiac remodelling. We highlight the important role that Wee1 plays as a mediator of cardiac remodelling via activating AKT–NFκB signalling pathway in cardiomyocytes. Importantly, we show that the activated Wee1 directly interacts with the PH domain of AKT to phosphorylate AKT. This finding identifies Wee1 as a potential therapeutic target for cardiac hypertrophy and remodelling.

Acknowledgements

We thank Scientific Research Center of Wenzhou Medical University for consultation and instrument availability that supported this work.

Supplementary data

Supplementary data are available at *European Heart Journal* online.

Declarations

Disclosure of Interest

All authors declare no disclosure of interest for this contribution..

Data Availability

The data underlying this article will be shared on reasonable request to the corresponding author.

Funding

This study was supported by the National Natural Science Foundation of China (82404625 to M.W., U24A20814 to G.L., and 82300532 to Z.X.) and the Key Discipline of Zhejiang Province in Public Health and Preventive Medicine (First Class, Category A) at Hangzhou Medical College.

Ethical Approval

All animal experimental protocols were approved by The Wenzhou Medical University Animal Policy and Welfare Committee approved all animal studies (Approval Document No: wydw 2021-1016). All experimental protocols using human heart tissues samples were approved by the Ethics Committee of Sir Run Run Shaw Hospital, School of Medicine, Zhejiang University (Ethics number: 2023-433-01).

Pre-registered Clinical Trial Number

Not applicable.

References

1. GBD 2016 Risk Factors Collaborators. Global, regional, and national comparative risk assessment of 84 behavioural, environmental and occupational, and metabolic risks or clusters of risks, 1990–2016: a systematic analysis for the Global Burden of Disease Study 2016. *Lancet* 2017;**390**:1345–422. https://doi.org/10.1016/s0140-6736(17)32366-8
2. Cleland JGF, Ferreira JP, Mariottoni B, Pellicori P, Cuthbert J, Verdonschot JAJ, *et al.* The effect of spironolactone on cardiovascular function and markers of fibrosis in people at increased risk of developing heart failure: the heart 'OMics' in AGEing (HOMAGE) randomized clinical trial. *Eur Heart J* 2021;**42**:684–96. https://doi.org/10.1093/eurheartj/ehaa758
3. Wang J, Gareri C, Rockman HA. G-protein-coupled receptors in heart disease. *Circ Res* 2018;**123**:716–35. https://doi.org/10.1161/circresaha.118.311403
4. Higashikuni Y, Liu W, Numata G, Tanaka K, Fukuda D, Tanaka Y, *et al.* NLRP3 inflammasome activation through heart-brain interaction initiates cardiac inflammation and hypertrophy during pressure overload. *Circulation* 2022;**147**:338–55. https://doi.org/10.1161/circulationaha.122.060860
5. Ardito F, Giuliani M, Perrone D, Troiano G, Lo Muzio L. The crucial role of protein phosphorylation in cell signaling and its use as targeted therapy (review). *Int J Mol Med* 2017;**40**:271–80. https://doi.org/10.3892/ijmm.2017.3036
6. Silnitsky S, Rubin S, Zerihun M, Qvit N. An update on protein kinases as therapeutic targets-part I: protein kinase C activation and its role in cancer and cardiovascular diseases. *Int J Mol Sci* 2023;**24**:17600. https://doi.org/10.3390/ijms242417600
7. Bossuyt J, Borst J, Verberckmoes M, Bailey L, Bers D, Hegyi B. Protein kinase D1 regulates cardiac hypertrophy, potassium channel remodeling, and arrhythmias in heart failure. *J Am Heart Assoc* 2022;**11**:e027573. https://doi.org/10.1161/jaha.122.027573
8. See F, Thomas W, Way K, Tzanidis A, Kompa A, Lewis D, *et al.* P38 mitogen-activated protein kinase inhibition improves cardiac function and attenuates left ventricular remodeling following myocardial infarction in the rat. *J Am Coll Cardiol* 2004;**44**:1679–89. https://doi.org/10.1016/j.jacc.2004.07.038
9. Shimizu T, Liao J. Rho kinases and cardiac remodeling. *Circ J* 2016;**80**:1491–8. https://doi.org/10.1253/circj.CJ-16-0433
10. Castelo-Soccio L, Kim H, Gadina M, Schwartzberg P, Laurence A, O'Shea J. Protein kinases: drug targets for immunological disorders. *Nat Rev Immunol* 2023;**23**:787–806. https://doi.org/10.1038/s41577-023-00877-7
11. Torre D, Lachmann A, Ma'ayan A. BioJupies: automated generation of interactive notebooks for RNA-Seq data analysis in the cloud. *Cell Syst* 2018;**7**:556–61.e3. https://doi.org/10.1016/j.cels.2018.10.007
12. Mueller S, Haas-Kogan DA. WEE1 kinase as a target for cancer therapy. *J Clin Oncol* 2015;**33**:3485–7. https://doi.org/10.1200/jco.2015.62.2290
13. Mahajan K, Mahajan N. WEE1 tyrosine kinase, a novel epigenetic modifier. *Trends Genet* 2013;**29**:394–402. https://doi.org/10.1016/j.tig.2013.02.003
14. Guo E, Xiao R, Wu Y, Lu F, Liu C, Yang B, *et al.* WEE1 inhibition induces anti-tumor immunity by activating ERV and the dsRNA pathway. *J Exp Med* 2021;**219**:e20210789. https://doi.org/10.1084/jem.20210789
15. Arang N, Kain H, Glennon E, Bello T, Dudgeon D, Walter E, *et al.* Identifying host regulators and inhibitors of liver stage malaria infection using kinase activity profiles. *Nat Commun* 2017;**8**:1232. https://doi.org/10.1038/s41467-017-01345-2
16. Tampakakis E, Gangrade H, Glavaris S, Htet M, Murphy S, Lin BL, *et al.* Heart neurons use clock genes to control myocyte proliferation. *Sci Adv* 2021;**7**:eabh4181. https://doi.org/10.1126/sciadv.abh4181
17. Iorns E, Lord CJ, Grigoriadis A, McDonald S, Fenwick K, Mackay A, *et al.* Integrated functional, gene expression and genomic analysis for the identification of cancer targets. *PLoS One* 2009;**4**:e5120. https://doi.org/10.1371/journal.pone.0005120
18. Harris PS, Venkataraman S, Alimova I, Birks DK, Balakrishnan I, Cristiano B, *et al.* Integrated genomic analysis identifies the mitotic checkpoint kinase WEE1 as a novel therapeutic target in medulloblastoma. *Mol Cancer* 2014;**13**:72. https://doi.org/10.1186/1476-4598-13-72
19. Fu S, Yao S, Yuan Y, Previs RA, Elias AD, Carvajal RD, *et al.* Multicenter phase II trial of the WEE1 inhibitor adavosertib in refractory solid tumors harboring CCNE1 amplification. *J Clin Oncol* 2022;**41**:1725–34. https://doi.org/10.1200/jco.22.00830
20. Gelinas R, Mailleux F, Dontaine J, Bultot L, Demeulder B, Ginion A, *et al.* AMPK activation counteracts cardiac hypertrophy by reducing O-GlcNAcylation. *Nat Commun* 2018;**9**:374. https://doi.org/10.1038/s41467-017-02795-4
21. Batlle M, Castillo N, Alcarraz A, Sarvari S, Sanguesa G, Cristobal H, *et al.* Axl expression is increased in early stages of left ventricular remodeling in an animal model with pressure-overload. *PLoS One* 2019;**14**:e0217926. https://doi.org/10.1371/journal.pone.0217926
22. Kunzel SR, Hoffmann M, Weber S, Kunzel K, Kammerer S, Gunscht M, *et al.* Diminished PLK2 induces cardiac fibrosis and promotes atrial fibrillation. *Circ Res* 2021;**129**:804–20. https://doi.org/10.1161/CIRCRESAHA.121.319425
23. Katayama K, Fujita N, Tsuruo T. Akt/protein kinase B-dependent phosphorylation and inactivation of WEE1Hu promote cell cycle progression at G2/M transition. *Mol Cell Biol* 2005;**25**:5725–37. https://doi.org/10.1128/mcb.25.13.5725-5737.2005
24. Ozes ON, Mayo LD, Gustin JA, Pfeffer SR, Pfeffer LM, Donner DB. NF-kappaB activation by tumour necrosis factor requires the Akt serine-threonine kinase. *Nature* 1999;**401**:82–5. https://doi.org/10.1038/43466
25. Do K, Doroshow JH, Kummar S. Wee1 kinase as a target for cancer therapy. *Cell Cycle* 2013;**12**:3159–64. https://doi.org/10.4161/cc.26062
26. Yu M, Qi B, Xiaoxiang W, Xu J, Liu X. Baicalein increases cisplatin sensitivity of A549 lung adenocarcinoma cells via PI3K/Akt/NF-κB pathway. *Biomed Pharmacother* 2017;**90**:677–85. https://doi.org/10.1016/j.biopha.2017.04.001
27. Zhang C, Peng K, Liu Q, Huang Q, Liu T. Adavosertib and beyond: biomarkers, drug combination and toxicity of WEE1 inhibitors. *Crit Rev Oncol Hematol* 2023;**193**:104233. https://doi.org/10.1016/j.critrevonc.2023.104233
28. Li C, Shen Q, Zhang P, Wang T, Liu W, Li R, *et al.* Targeting MUS81 promotes the anticancer effect of WEE1 inhibitor and immune checkpoint blocking combination therapy via activating cGAS/STING signaling in gastric cancer cells. *J Exp Clin Cancer Res* 2021;**40**:315. https://doi.org/10.1186/s13046-021-02120-4
29. Wang B, Sun L, Yuan Z, Tao Z. Wee1 kinase inhibitor AZD1775 potentiates CD8+ T cell-dependent antitumour activity via dendritic cell activation following a single high dose of irradiation. *Med Oncol* 2020;**37**:66. https://doi.org/10.1007/s12032-020-01390-w
30. Nakada Y, Nhi Nguyen NU, Xiao F, Savla JJ, Lam NT, Abdisalaam S, *et al.* DNA damage response mediates pressure overload-induced cardiomyocyte hypertrophy. *Circulation* 2019;**139**:1237–9. https://doi.org/10.1161/CIRCULATIONAHA.118.034822
31. McCalmon SA, Desjardins DM, Ahmad S, Davidoff KS, Snyder CM, Sato K, *et al.* Modulation of angiotensin II-mediated cardiac remodeling by the MEF2A target gene Xirp2. *Circ Res* 2010;**106**:952–60. https://doi.org/10.1161/CIRCRESAHA.109.209007
32. Wu X, Zhou X, Wang S, Mao G. DNA damage response(DDR): a link between cellular senescence and human cytomegalovirus. *Virol J* 2023;**20**:250. https://doi.org/10.1186/s12985-023-02203-y
33. Saul D, Jurk D, Doolittle ML, Kosinsky RL, Monroe DG, LeBrasseur NK, *et al*. Distinct secretomes in p16- and p21- positive senescent cells across tissues. *bioRxiv*, https://doi.org/10.1101/2023.12.05.569858, 5 December 2023, preprint: not peer reviewed.
34. Zhu X, Su Q, Xie H, Song L, Yang F, Zhang D, *et al.* SIRT1 deacetylates WEE1 and sensitizes cancer cells to WEE1 inhibition. *Nat Chem Biol* 2023;**19**:585–95. https://doi.org/10.1038/s41589-022-01240-y
35. Liu Y, Zhang G, Yang Y, Zhang C, Fu R, Yang Y. Genistein induces G2/M arrest in gastric cancer cells by increasing the tumor suppressor PTEN expression. *Nutr Cancer* 2013;**65**:1034–41. https://doi.org/10.1080/01635581.2013.810290
36. Zhu C, Yuan T, Krishnan J. Targeting cardiomyocyte cell cycle regulation in heart failure. *Basic Res Cardiol* 2024;**119**:349–69. https://doi.org/10.1007/s00395-024-01049-x
37. Alvarez R Jr, Wang BJ, Quijada PJ, Avitabile D, Ho T, Shaitrit M, *et al.* Cardiomyocyte cell cycle dynamics and proliferation revealed through cardiac-specific transgenesis of fluorescent ubiquitinated cell cycle indicator (FUCCI). *J Mol Cell Cardiol* 2019;**127**:154–64. https://doi.org/10.1016/j.yjmcc.2018.12.007
38. Fang J, de Bruin A, Villunger A, Schiffelers R, Lei Z, Sluijter JPG. Cellular polyploidy in organ homeostasis and regeneration. *Protein Cell* 2023;**14**:560–78. https://doi.org/10.1093/procel/pwac064
39. Kadatane SP, Satariano M, Massey M, Mongan K, Raina R. The role of inflammation in CKD. *Cells* 2023;**12**:1581. https://doi.org/10.3390/cells12121581
40. Aime-Sempe C, Folliguet T, Rucker-Martin C, Krajewska M, Krajewska S, Heimburger M, *et al.* Myocardial cell death in fibrillating and dilated human right atria. *J Am Coll Cardiol* 1999;**34**:1577–86. https://doi.org/10.1016/s0735-1097(99)00382-4
41. Ghafouri-Fard S, Khanbabapour Sasi A, Hussen BM, Shoorei H, Siddiq A, Taheri M, *et al.* Interplay between PI3K/AKT pathway and heart disorders. *Mol Biol Rep* 2022;**49**:9767–81. https://doi.org/10.1007/s11033-022-07468-0
42. Cheng Y, Shen A, Wu X, Shen Z, Chen X, Li J, *et al.* Qingda granule attenuates angiotensin II-induced cardiac hypertrophy and apoptosis and modulates the PI3K/AKT pathway. *Biomed Pharmacother* 2021;**133**:111022. https://doi.org/10.1016/j.biopha.2020.111022
43. Hsieh P-L, Chu P-M, Cheng H-C, Huang Y-T, Chou W-C, Tsai K-L, *et al.* Dapagliflozin mitigates doxorubicin-caused myocardium damage by regulating AKT-mediated oxidative stress, cardiac remodeling, and inflammation. *Int J Mol Sci* 2022;**23**:10146. https://doi.org/10.3390/ijms231710146
44. DeBosch B, Treskov I, Lupu T, Weinheimer C, Kovacs A, Courtois M, *et al.* Akt1 is required for physiological cardiac growth. *Circulation* 2006;**113**:2097–104. https://doi.org/10.1161/circulationaha.105.595231

45. Zhang X, Jin B, Huang C. The PI3K/Akt pathway and its downstream transcriptional factors as targets for chemoprevention. *Curr Cancer Drug Targets* 2007;**7**:305–16. https://doi.org/10.2174/156800907780809741
46. Tuo P, Zhao R, Li N, Yan S, Yang G, Wang C, *et al.* Lycorine inhibits Ang II-induced heart remodeling and inflammation by suppressing the PI3K-AKT/NF-κB pathway. *Phytomedicine* 2024;**128**:155464. https://doi.org/10.1016/j.phymed.2024.155464
47. Ke Z, Wang G, Yang L, Qiu H, Wu H, Du M, *et al.* Crude terpene glycoside component from Radix paeoniae rubra protects against isoproterenol-induced myocardial ischemic injury via activation of the PI3K/AKT/mTOR signaling pathway. *J Ethnopharmacol* 2017;**206**:160–9. https://doi.org/10.1016/j.jep.2017.05.028
48. Doukas J, Wrasidlo W, Noronha G, Dneprovskaia E, Fine R, Weis S, *et al.* Phosphoinositide 3-kinase gamma/delta inhibition limits infarct size after myocardial ischemia/reperfusion injury. *Proc Natl Acad Sci U S A* 2006;**103**:19866–71. https://doi.org/10.1073/pnas.0606956103
49. Chen O, Cao Z, Li H, Ye Z, Zhang R, Zhang N, *et al.* High-concentration hydrogen protects mouse heart against ischemia/reperfusion injury through activation of thePI3K/Akt1 pathway. *Sci Rep* 2017;**7**:14871. https://doi.org/10.1038/s41598-017-14072-x
50. Enomoto M, Goto H, Tomono Y, Kasahara K, Tsujimura K, Kiyono T, *et al.* Novel positive feedback loop between Cdk1 and Chk1 in the nucleus during G2/M transition. *J Biol Chem* 2009;**284**:34223–30. https://doi.org/10.1074/jbc.C109.051540
51. Guerau-de-Arellano M, Piedra-Quintero Z, Tsichlis P. Akt isoforms in the immune system. *Front Immunol* 2022;**13**:990874. https://doi.org/10.3389/fimmu.2022.990874
52. Milburn C, Deak M, Kelly S, Price N, Alessi D, Van Aalten D. Binding of phosphatidylinositol 3,4,5–trisphosphate to the pleckstrin homology domain of protein kinase B induces a conformational change. *Biochem J* 2003;**375**:531–8. https://doi.org/10.1042/bj20031229
53. Truebestein L, Hornegger H, Anrather D, Hartl M, Fleming K, Stariha J, *et al.* Structure of autoinhibited Akt1 reveals mechanism of PIP-mediated activation. *Proc Natl Acad Sci U S A* 2021;**118**:e2101496118. https://doi.org/10.1073/pnas.2101496118
54. Vassilopoulos A, Tominaga Y, Kim H, Lahusen T, Li B, Yu H, *et al.* WEE1 murine deficiency induces hyper-activation of APC/C and results in genomic instability and carcinogenesis. *Oncogene* 2015;**34**:3023–35. https://doi.org/10.1038/onc.2014.239
55. Hirai H, Iwasawa Y, Okada M, Arai T, Nishibata T, Kobayashi M, *et al.* Small-molecule inhibition of Wee1 kinase by MK-1775 selectively sensitizes p53-deficient tumor cells to DNA-damaging agents. *Mol Cancer Ther* 2009;**8**:2992–3000. https://doi.org/10.1158/1535-7163.Mct-09-0463
56. Aarts M, Sharpe R, Garcia-Murillas I, Gevensleben H, Hurd M, Shumway S, *et al.* Forced mitotic entry of S-phase cells as a therapeutic strategy induced by inhibition of WEE1. *Cancer Discov* 2012;**2**:524–39. https://doi.org/10.1158/2159-8290.Cd-11-0320
57. Geenen JJJ, Schellens JHM. Molecular pathways: targeting the protein kinase wee1 in cancer. *Clin Cancer Res* 2017;**23**:4540–4. https://doi.org/10.1158/1078-0432.CCR-17-0520

Correction

https://doi.org/10.1093/eurheartj/ehaf529
Online publish-ahead-of-print 22 July 2025

Correction to: Immune checkpoint inhibitor-associated myocarditis: a novel risk score

This is a correction to: John R Power, Charles Dolladille, Benay Ozbay, Adrien Procureur, Stephane Ederhy, Nicolas L Palaskas, Lorenz H Lehmann, Jennifer Cautela, Pierre-Yves Courand, Salim S Hayek, Han Zhu, Vlad G Zaha, Richard K Cheng, Joachim Alexandre, François Roubille, Lauren A Baldassarre, Yen-Chou Chen, Alan H Baik, Michal Laufer-Perl, Yuichi Tamura, Aarti Asnani, Sanjeev Francis, Elizabeth M Gaughan, Peter P Rainer, Guillaume Bailly, Danette Flint, Dimitri Arangalage, Eve Cariou, Roberta Florido, Anna Narezkina, Yan Liu, Shahneen Sandhu, Darryl Leong, Nahema Issa, Nicolas Piriou, Lucie Heinzerling, Giovanni Peretto, Shanthini M Crusz, Nausheen Akhter, Joshua E Levenson, Isik Turker, Assié Eslami, Charlotte Fenioux, Pedro Moliner, Michel Obeid, Wei Ting Chan, Stephen M Ewer, Seyed Ebrahim Kassaian, Douglas B Johnson, Anju Nohria, Osnat Itzhaki Ben Zadok, Javid J Moslehi, Joe-Elie Salem, International ICI-Myocarditis Registry, on behalf of, Immune checkpoint inhibitor-associated myocarditis: a novel risk score, *European Heart Journal*, Volume 47, Issue 9, 1 March 2026, Pages 1050–1062, https://doi.org/10.1093/eurheartj/ehaf315

In the originally published version of this manuscript, the names of the following collaborating authors were omitted from the Appendix section:

Yves Allenbach, Sonali Rao, Thomas Similowski, Anja Karlstaedt.

This has been corrected in the article.